Science of the Total Environment 785 (2021) 147370

Contents lists available at ScienceDirect

Science of the Total Environment

journal homepage: www.elsevier.com/locate/scitotenv

Reproductive toxicity and metabolic perturbations in male rats exposed to boron

Chong Wang [a], Ziqing Kong [b], Lian Duan [a], Fuchang Deng [a], Yuanyuan Chen [a], Sheng Quan [b], Xiaohui Liu [c], Yu'e Cha [a], Yufeng Gong [d], Chao Wang [a,d], Ying Shi [a], Wen Gu [a], Yuanzheng Fu [a], Donghai Liang [e], John P. Giesy [d,f,g], Hongwei Zhang [a], Song Tang [a,h,*]

[a] China CDC Key Laboratory of Environment and Population Health, National Institute of Environmental Health, Chinese Center for Disease Control and Prevention, Beijing 100021, China
[b] Calibra-Metabolon Joint Metabolomics Laboratory, Calibra Diagnostics, Ltd., Hangzhou, Zhejiang 310000, China
[c] National Protein Science Technology Center and School of Life Sciences, Tsinghua University, Beijing 100084, China
[d] Toxicology Centre, University of Saskatchewan, Saskatoon, SK S7N 5B3, Canada
[e] Gangarosa Department of Environmental Health, Rollins School of Public Health, Emory University, Atlanta, GA 30322, USA
[f] Department of Biomedical and Veterinary Biosciences, University of Saskatchewan, Saskatoon, SK S7N 5B4, Canada
[g] Department of Environmental Science, Baylor University, Waco, TX 76798, USA
[h] Center for Global Health, School of Public Health, Nanjing Medical University, Nanjing, Jiangsu 211166, China

HIGHLIGHTS

- Boron (B) exposure significantly affected male rat reproductive fitness by reducing live foetus proportion
- B significantly increased rat testicular enzymes of MDH and G3PDH as well as plasma FSH
- B significantly increased rat testicular steroid hormones of ASD, DHEA, E_1, E_2, E_3, and T
- B significantly reduced the levels of testicular SDH and plasma IL-5
- Metabolomics/lipidomics revealed that B remodeled metabolisms of lipids and amino acids

GRAPHICAL ABSTRACT

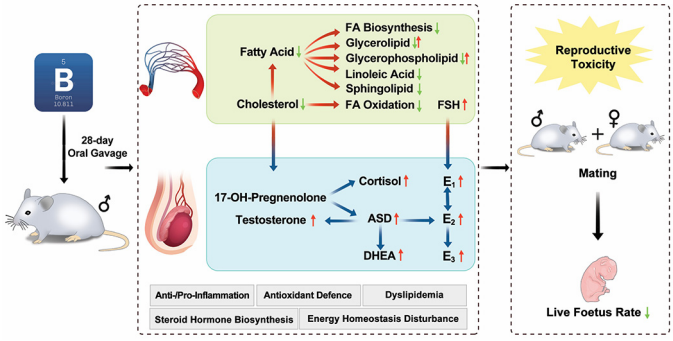

ARTICLE INFO

Article history:
Received 8 January 2021
Received in revised form 22 April 2021
Accepted 22 April 2021
Available online 28 April 2021

Editor: Lotfi Aleya

Keywords:
Seawater desalination
Boron
Male reproduction
Metabolomics

ABSTRACT

The poor rejection of boron (B) by reverse osmosis, a dominant seawater desalination and household-scale water treatment technology, is a critical issue given its potential adverse effects on human health and the extensive and increasing application of seawater desalination facilities worldwide. Although previous in vivo studies have revealed the reproductive toxicity of B, the mechanistic underpinnings and changes in the global metabolome remains undefined. To systematically investigate the effects of B on male reproduction and endogenous metabolic fingerprints, adult male rats were exposed to different doses of borax (25, 50 and 100 mg B/kg/day) for 28 days via oral gavage. After mating the treated rats with untreated female rats, we found a significant reduction in the proportion of live foetuses only in the highest dose group (100 mg B/kg/day) compared with the control group (treated with deionised water). Furthermore, compared with the control group, the concentration of plasma follicle-stimulating hormone increased and the activities of testicular enzymes (malate dehydrogenase and glyceraldehyde-3-phosphate dehydrogenase) were significantly upregulated in the 100 mg B/kg/day group, whereas the activity of testicular sorbitol dehydrogenase and the concentrations of plasma interleukin-5 were inversely proportional to the doses and were the lowest at the highest dose of 100 mg B/kg/day. The concentrations

* Corresponding author at: No. 7 Panjiayuan Nanli, Chaoyang District, Beijing 100021, China.
E-mail address: tangsong@nieh.chinacdc.cn (S. Tang).

https://doi.org/10.1016/j.scitotenv.2021.147370
0048-9697/© 2021 Elsevier B.V. All rights reserved.

Lipidomics
Pathway analysis

of testicular hormones (e.g., oestrone, oestradiol, oestriol, testosterone, cortisol and androstenedione) were significantly upregulated in the rats exposed to 100 mg B/kg/day. Non-targeted metabolomics and lipidomics revealed a significant disruption of lipid and amino acids metabolism at the highest dose, particularly that of linoleic acid, α-linolenic acid, sphingolipid, glycerolipid, glycerophospholipid, branched-chain amino acid and nicotinate metabolism, and unsaturated fatty acids synthesis, which are predominantly associated with inflammation, antioxidation defence, energy utilisation, steroid hormone synthesis and lipid abnormalities. Our results offer insights into the mechanisms underlying the adverse effects of B on reproduction and into the health risks posed by drinking desalinated seawater that containing elevated B concentrations.

© 2021 Elsevier B.V. All rights reserved.

1. Introduction

With high population growth, rapid industrialisation, rapid urbanisation and climate change, the need for secure sources of clean drinking water is increasing and shortages are becoming increasingly acute. To offset these deficiencies, desalination of seawater and brackish groundwater has been rapidly developed and considered as a viable option to meet the increasing global demands for freshwater (Schiermeier, 2008). As of 30 June 2018, more than 20,000 desalination plants in 150 countries, including the United States, Europe, China and the Gulf Cooperation Council countries, produced 86.8 million m^3/day of drinking water. They were expected to produce 120 million m^3/day in 2020 (Aquatech, 2019). In 2018, approximately 1% of the global population drank desalinated seawater (Sedlak, 2019). Although the primary intention of desalination is to remove natural ionic minerals, boron (B) removed by reverse osmosis (RO), a dominant seawater desalination and household-scale water treatment technology, is insufficient. Boron generally exists as non-dissociated, neutrally charged and small-molecular mass boric acid, which can freely diffuse through RO membranes (Breitner et al., 2018), thereby resulting in 2–3 mg/L of B in the desalinated seawater intended for drinking and agricultural irrigation. This is higher than the permissible limits of the Standards for Drinking Water Quality of China (0.50 mg B/L) and those for crops (0.50–0.75 mg/L) (NHC.PRC, 2020; Vera et al., 2019).

Boron is a rare element but is widely distributed in the Earth's crust (Howe, 1998; Murray, 1995). It is not present as a single element in nature, and is always found in the form of more than 200 minerals with different amounts of calcium, sodium or magnesium. Borax is the most commonly form of B (Wolska and Bryjak, 2013) and is extensively used as a cleaner and in household products, herbicides, and paints, thereby contributing to anthropogenic sources of B (Kabu and Akosman, 2013). Borax concentrations in surface water are typically less than 1 mg B/L, whereas those in marine waters are approximately 4.6 mg B/L (Nan et al., 2018). The B concentrations in drinking water in Chinese cities range from 0.001 mg B/L to 1.880 mg B/L (Zhang et al., 2012). Given the natural occurrence, ubiquity and extensive use of B and the increasing application of RO desalination worldwide, humans and animals exposure to B is unavoidable. Thus, investigation of the unintended adverse consequences of B is exposure to have global significance.

Boron is a trace element with an important role in various physiological processes (Hunt and Idso, 1999; Nielsen, 1998; Nielsen and Penland, 1999; Penland, 1998), including cell membrane function, mineral and lipid metabolism, energy utilisation, and immune system function (Cui et al., 2004; Goldbach and Wimmer, 2007; Hammes and Wu, 1971; Hu et al., 2014; Miwa et al., 2007; Rajendran et al., 1995; Tanaka and Fujiwara, 2008). Although an appropriate amount of B is considered 'probably essential' for humans by the World Health Organization (BCS, 2013), too little or too much B might cause adverse effects. Excessive B intake can affect reproductive fitness and developmental function in experimental animals (U.S. EPA, 2002).

Many in vivo studies of B have revealed that the testis is the primary target organ in male rats and mice. Testicular atrophy/pathology, plasma hormones [e.g. follicle-stimulating hormone (FSH) and luteinising hormone (LH)] and testicular enzymes were changed in a time-dependent and dose-dependent manner (Dixon et al., 1979; Lee et al., 1978; Linnder et al., 1990; Treinen and Chapin, 1991). For example, F344 rats administered with a dose of 450 mg B/kg/day for 28 days showed testicular tissue lesions, decreased spermiation, and testicular atrophy (Aktas et al., 2020). Sprague-Dawley rats dietary exposed to borax (35 and 50 mg B/kg/day) showed time-dependent and dose-dependent decreases in plasma FSH and LH concentrations. In human studies, B has been shown to increase blood levels of steroid hormones [e. g., 17-beta-estradiol (E2) and testosterone (T)] in women and men with B supplementation (Abdelnour et al., 2018; Khaliq et al., 2018). However, an occupationally exposed population study showed the adverse effects of B on semen parameters, but reported no changes in the FSH, LH and total T concentrations, even in the extreme exposure group (Duydu et al., 2018a, b). Another large-scale human study showed that the biomarkers of oxidative stress and immune function-related interleukins (IL-6 and IL-8) and nuclear factor kappa B failed to change, but changes in these parameters were observed in animals (Başaran et al., 2020). The apparent contradictory results between humans and animals could be explained by the fact that the B concentrations that induce reproductive toxicity in humans are not be reached even with the most extreme occupational exposures (Bolt et al., 2020; Duydu et al., 2011; Duydu et al., 2018a; Duydu et al., 2018b; Robbins et al., 2010). The mean blood B concentration in humans with high exposure was much lower than that in rats with developmental or reproductive toxicities (Duydu et al., 2012a, 2012b; Farfán-García et al., 2016). Therefore, taking into account of the effective dose, there is no contradiction between human results and animal experimental findings of B-induced reproductive toxicity (Bolt et al., 2020).

Metabolomics, a powerful tool that systematically analyses small-molecule phenotypes, can be used to investigate global metabolic responses to abiotic or biotic stressors and is useful for tracking subtle changes in organisms (Bundy et al., 2009; Liang et al., 2018; Zhao et al., 2017). Lipids are critical for diverse biological functions including membrane structure and function, signalling, energy storage, and immune system response (Han, 2016; Nguyen et al., 2017). Lipidomics is a promising method for integral investigation of the changes in lipids as a biological response to stressor stimuli (Gao et al., 2019; Han, 2016; Zhang et al., 2019). Boron-induced responses of endogenous metabolites have not been investigated in vivo. In this study, we hypothesized that the male reproductive toxicity induced by B exposure might be mediated through the alternations in testicular enzyme levels, steroid hormone homeostasis, and metabolic profiling. To this end, male rats were administered to borax by oral gavage for 28 consecutive days, and a comprehensive examination was conducted afterwards. Specifically, 1) the reproductive toxicity was measured via a fertility assessment and a histoarchitectural assessment of testis and epididymis; 2) the levels of testicular enzymes [e.g. hyaluronidase (H), sorbitol dehydrogenase (SDH), glyceraldehyde-3-phosphote dehydrogenase (G3PDH) and malate dehydrogenase (MDH)] and testicular steroid hormones [e.g., oestrone (E_1), E_2, oestriol (E_3), T and cortisol] were analysed. 3) a series of plasma cytokines and gonadotropin (e.g. LH and FSH) were examined; and 4) we combined metabolomics and lipidomics for the first time owing to their non-targeted and holistic

features to measure the changes in plasma metabolites and relevant metabolic pathways to explore the metabolic perturbations associated with B-induced toxicity (Gu et al., 2018).

2. Materials and methods

2.1. Chemicals and materials

Because B does not exist in a free state in nature, borax ($Na_2B_4O_7 \cdot 10H_2O$, CAS 1303-96-4, 99.5% purity), the most popular commercial form of B, was used (Sigma-Aldrich, St. Louis, MO, USA). The borax dose was expressed in terms of B equivalent as follows: borax dose×0.113 = equivalent B dose (U.S. EPA, 2008a). The chemicals and kits are described in detail in the Supporting Information (SI).

2.2. Animals and boron exposure

Pathogen-free adult male ($n = 68$) and female ($n = 200$) Sprague-Dawley rats weighing 250–300 g were obtained from Jinmuyang Experimental Animal Breeding Co., Ltd. (Beijing, China) and housed in the Experimental Animal Center of the Chinese Center for Disease Control and Prevention (China CDC). All of the animal procedures were approved by the Institutional Animal Care and Use Committee (No. 2016007).

After 1 week of acclimation, the male rats were weighted and randomly divided into four groups (three exposure groups and one control group; $n = 17$ in each group). The rats in the exposure groups were administrated 25, 50 or 100 mg B/kg diluted with deionised water once per day by oral gavage for 28 consecutive days, whereas those in the control group were administered deionised water. The doses were selected based on the no-observed-adverse-effect level (25 mg B/kg/day) of testicular toxicity in male rats (U.S. EPA, 2008b). Five live rats from each group were used for the male fertility test, whereas the remaining 12 rats were anaesthetised at 28 days (Dixon et al., 1979; Lee et al., 1978). Eight of the 12 male rats were used for blood (plasma) collection to determine testicular steroid hormones, cytokines, metabolomics and lipidomics, and the remaining four rats were used to analyse testicular enzyme levels and pathological changes. The organs (testes and epididymides) were removed immediately and weighed separately. The left testis and paired epididymis were fixed for histopathological examination. The right testis was immediately placed at −80 °C for testicular enzymes determination. The animal exposure procedure is described in detail in the SI.

2.3. Boron quantification

Boron concentrations were determined in the testis, diet, plasma, and water samples using an inductively coupled plasma mass spectrometer (iCAP RQ ICP-MS, Thermo Fisher, Waltham, MA, USA). The assay details are provided in the SI.

2.4. Male fertility assay

After 28 days of exposure, the remaining five male rats in each group were caged individually with an untreated virgin proestrus female rat and housed together in at a 1:1 ratio for a 7-day mating period. The serial fertility and gestation processes were repeated 10 times, lasting for a total of 10 weeks. The assay details are provided in the SI.

2.5. Analyses of testicular enzymes, testicular steroid hormones, plasma hormones and plasma cytokines

Plasma FSH and LH ($n = 8$) and testicular SDH, MDH, G3PDH, H, E_1, E_2, E_3, T, cortisol, 25-hydroxyvitamin D_3 (25[OH]D_3), dehydroepiandrosterone (DHEA), androstenedione (ASD) or aldosterone (ALD) ($n = 4$) were determined using ELISA kits (Wuhan Colorful Gene Biological Technology Company, Wuhan, China) following the manufacturer's instructions. The Rat Cytokine/Chemokine 15-Plex Panel was used to measure interleukins (IL-1α, IL-1β, IL-2, IL-4, IL-5, IL-12 and IL-17), interferon gamma (IFN-γ), colony-stimulating factors (G-CSF and GM-CSF), growth factors [epidermal growth factor and vascular endothelial growth factor A (VEGF-A)], and chemokines (IP-10, RANTES/CCL5 and Eotaxin/CCL11], while the Metabolic Hormone 9-Plex Panel (Billerica, MA, USA) was used to measure IL-6, tumor necrosis factor (TNF-γ), monocyte chemoattractant protein-1, metabolic hormones (leptin, insulin, pancreatic polypeptide, peptide YY, gastric inhibitory peptide, and C-peptide) in 25 μL of plasma ($n = 5$). The assay details are provided in the SI.

2.6. Metabolomics, lipidomics and data processing

After 28 days of exposure, non-targeted metabolomics of 100 μL of plasma ($n = 5$) was performed at the Calibra-Metabolon Joint Metabolomics Laboratory (Hangzhou, Zhejiang, China) using a Waters ACQUITY ultra-performance liquid chromatography (UPLC) and a Q-Exactive high- resolution/accurate mass spectrometer (Thermo Fisher, Waltham, MA, USA). Lipidomics of 100 μL of plasma ($n = 5$) was performed using a Q-Exactive Orbitrap with an XSelect CSH C18 column. Chromatographic conditions, compound identification, and quality assurance/quality control (QC) procedures are described in detail in the SI. Metabolomics/lipodomics data have been deposited into CNGB Sequence Archive (CNSA) of China National GeneBank DataBase (CNGBdb) with an accession No. CNP0001732 (https://db.cngb.org/cnsa/).

2.7. Data analysis

Statistical analyses were performed using R software v3.3.1 (R Foundation for Statistical Computing, Vienna, Austria. https://www.R-project.org/). The statistical differences between the control and exposures groups were evaluated by a one-way analysis of variance and Student's *t*-test or chi-square test. After normalisation, metabolic peaks were imported into R for partial least squares discriminant analysis (PLS-DA) using *mixOmics* and *ggplot2* packages. A multivariate statistical analysis (pairwise Adonis; $n = 9999$) was used to examine the changes in the metabolites in the exposure groups. Welch's two-sample *t*-test was used to identify significantly different metabolites between the experimental groups. An estimate of the false discovery rate (FDR) was calculated using the Benjamin-Hochberg method ($FDR_{B\text{-}H}$).

A pathway enrichment analysis was performed for significantly changed metabolites and lipids using MetaboAnalyst 4.0 (https://www.metaboanalyst.ca/), which is a comprehensive platform dedicated for metabolomics data analyses (Chong et al., 2019). This analysis requires the compound name or human metabolome database (HMDB) for each metabolite. A chemical similarity analysis of significantly changed metabolites and lipids at 100 mg B/kg/day was performed using ChemRICH (http://chemrich.fiehnlab.ucdavis.edu), which utilises structure similarity and chemical ontologies to map all known metabolites and name metabolic modules (Barupal and Fiehn, 2017). The compound name, InChiKeys, PubChem ID, SMILES, *p*-value and fold change for each metabolite are required for this analysis.

3. Results

3.1. Changes in body and organ weights

Of the male rats receiving B by oral gavage at the doses of 25, 50 and 100 mg/kg/day for 28 days, only those receiving 100 mg B/kg/day showed a significant decrease in body weight at 1 week and 2 weeks compared with the control group (Table S1). Except for a decrease in the ratio of heart and body weight (Table S2), no significant changes in mortality, the body growth rate or organ weights (e.g. testes and

epididymides) were found at 28 days in any exposure group in comparison with the control group. Moreover, no significant pathological changes in the seminiferous tubular diameter or number of spermatogonia and primary spermatocytes were found after exposure at any dose (Table S3 and Fig. S1).

3.2. Boron contents in the plasma and testes

After 28 days of exposure to 0 (deionised water: control), 25, 50 and 100 mg B/kg/day, the plasma B concentrations were 30, 133, 243, and 422 μg/L, respectively, thereby indicating a dose-dependent increase in B bioaccumulation (Fig. 1A and Table S4). However, no significant differences were observed in the testicular B contents between the groups (Fig. 1E and Table S4).

3.3. Assessment of male fertility

Although B had no effect on the gestation rate of pregnant female rats and the average number of foetuses after 10 mating periods, an effect on foetal abnormality was observed (Table 1). Specifically, at exposure doses of 50 and 100 mg B/kg/day, the live-foetus rates significantly decreased after the first 2 weeks, and then reached normal values after 3 weeks.

3.4. Changes in testicular enzymes and steroid hormones

The effects of B on G3PDH, MDH and SDH, enzymes that are associated with post-meiotic spermatogenic cells, are presented in Figs. 1F-H. Compared with the control group, the SDH activity in the B exposure groups significantly decreased in a dose-dependent manner, whereas the G3PDH and MDH activities significantly increased in the 100 mg B/kg/day exposure group ($p < 0.05$). As shown in Fig. 2, the concentrations of testicular 25[OH]D_3, ASD, cortisol, E_1, E_2, E_3, and T were significantly upregulated in a dose-dependent manner, especially in the 100 mg B/kg/day group compared with control group ($p < 0.05$). The concentrations of ASD and E_2 were significantly increased in all of the exposure groups (25, 50 and 100 mg B/kg/day) compared with the control group (Fig. 2B and 2F). The DHEA concentration was significantly elevated in the 25 and 50 mg B/kg/day groups (Fig. 2D), whereas the ALD concentration was significantly increased only in the 50 mg B/kg/day group ($p < 0.01$) (Fig. S2).

3.5. Changes in plasma hormones and cytokines

The plasma FSH concentration in the B exposure groups significantly increased in a dose-response manner ($p < 0.05$) (Fig. 1D). However, the plasma LH concentration did not change with the increase in dose (Fig. S2). To further explore the effects of B on immune and endocrine functions, the plasma concentrations of 24 cytokines and metabolic hormones were measured (Figs. 1 and S2). Among them, only IL-5 and VEGF concentrations exhibited significant changes. Specifically, the IL-5 concentration was significantly lower in the 100 mg B/kg/day group than in the control group (Fig. 1B). Exposure to 50 mg B/kg/day significantly promoted the secretion of VEGF in the rats (Fig. 1C), but exposure to the higher dose of 100 mg B/kg/day led to no changes in the VEGF concentration in comparison with the control group.

3.6. Changes in global metabolites

The median relative standard deviations for pooled QC samples were 7.0% and 3.6% for metabolomics and lipidomics, respectively. The PLS-DA results of the similarities and differences in the global metabolome and lipidome profiles between the control and exposure groups are presented in Figs. 3A,B. Exposure to higher doses of B for 28 days tended to drive an increasing difference from the control, with the highest dose of 100 mg B/kg/day resulting in the greatest difference from the control group.

In total, 691 plasma metabolic features and 502 plasma lipids of known identity were found based on accurate mass, retention time and tandem mass spectrometry (MS/MS) fragment matching

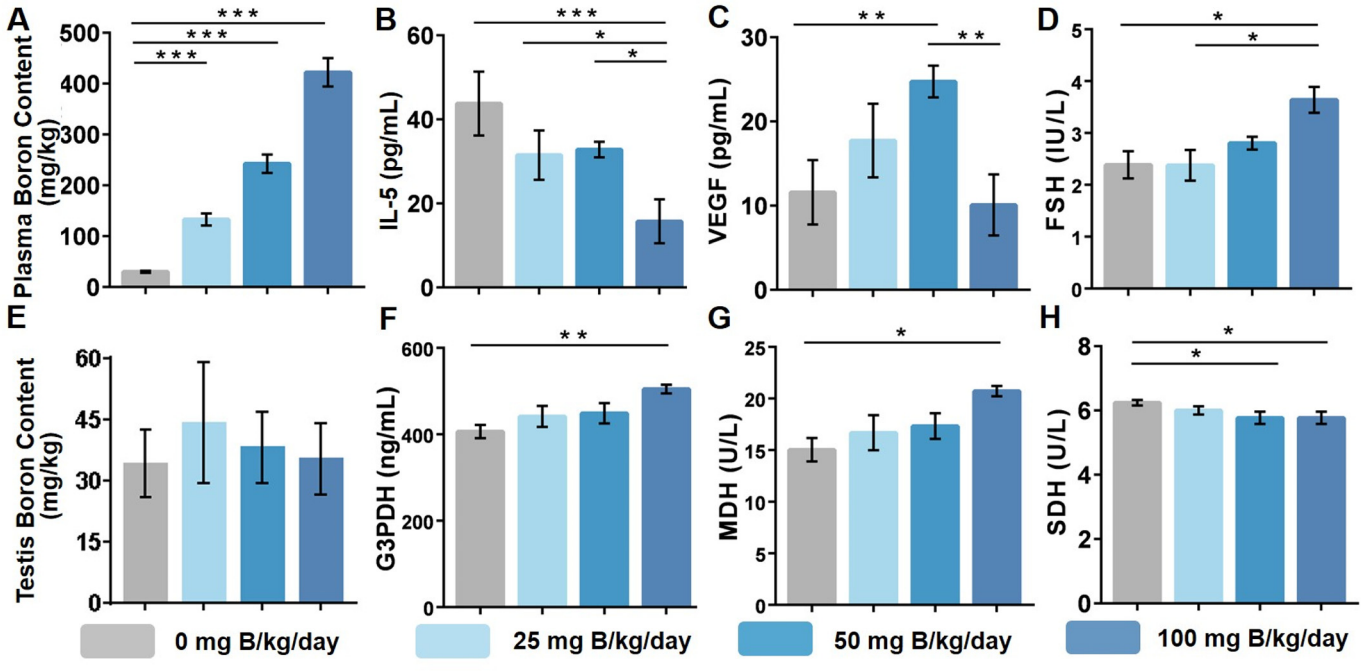

Fig. 1. Changes in plasma boron (A), cytokines of interleukin-5 (IL-5) (B) and vascular endothelial growth factor (VEGF) (C), gonadotropin of follicle-stimulating hormone (FSH) (D), testis boron (E), testicular enzymes of glycerol-3-phosphate dehydrogenase (G3PDH) (F), malate dehydrogenase (MDH) (G), and sorbitol dehydrogenase (SDH) (H) in male rats exposed to 0, 25, 50 and 100 mg B/kg/day for 28 days. Different colours indicate the samples ($n = 4$ or 5) are from different groups. Data are presented as the mean and standard error of the mean. Significance was determined at $p < 0.05^{*}$, $p < 0.01^{**}$ and $p < 0.001^{***}$ by Student's *t*-test.

Table 1
Effects of 0, 25, 50 and 100 mg B/kg/day exposure for 28 days on male rat fertility. After exposure, one male rat ($n = 5$) was paired with an untreated virgin proestrus female rat and housed together at a 1:1 ratio for a 1-week mating period. The serial fertility and gestation process were repeated 10 times and lasted for 10 weeks. Fertility data were obtained by calculating the percentage of pregnant female rats ($n = 5$) at the end of each mating period.

Time (week)	Gestation rate (%)				Mean number of foetuses				Proportion of live foetuses (%)			
	0	25	50	100	0	25	50	100	0	25	50	100
1	100 (5/5)	100 (5/5)	60 (3/5)	60 (3/5)	13.8 (69/5)	14.4 (72/5)	13.7(41/3)	16 (48/3)	100 (69/69)	95.8 (69/72)	82.9 (34/41)***	85.4 (41/48)**
2	100 (5/5)	100 (5/5)	80 (4/5)	80 (4/5)	15.4 (77/5)	14 (70/5)	15 (60/4)	14.3 (57/4)	100 (77/77)	100 (70/70)	93.3 (56/60)*	85.9 (49/57)***
3	100 (5/5)	100 (5/5)	60 (3/5)	100 (5/5)	13.4 (67/5)	14.8 (74/5)	14.7 (44/3)	13.8 (69/5)	98.5 (66/67)	100 (74/74)	100 (44/44)	100 (69/69)
4	100 (5/5)	100 (5/5)	100 (5/5)	100 (5/5)	13.4 (67/5)	13.8 (69/5)	13.2 (66/5)	14.2 (71/5)	100 (67/67)	98.5 (68/69)	93.9 (62/66)	94.3 (67/71)
5	100 (5/5)	100 (5/5)	100 (5/5)	100 (5/5)	14.8 (74/5)	10.8 (54/5)	15 (75/5)	8.8 (44/5)	94.6 (70/74)	92.6 (50/54)	93.3 (70/75)	95.4 (42/44)
6	100 (5/5)	100 (5/5)	100 (5/5)	100 (5/5)	12.4 (62/5)	11.4 (57/5)	13.8 (69/5)	13 (65/5)	98.4 (61/62)	96.5 (55/57)	95.6 (66/69)	100 (50/50)
7	100 (5/5)	100 (5/5)	100 (5/5)	100 (5/5)	13 (65/5)	13 (65/5)	13 (65/5)	13 (65/5)	96.9 (63/65)	95.4 (62/65)	98.5 (64/65)	96.9 (63/65)
8	100 (5/5)	100 (5/5)	100 (5/5)	100 (5/5)	14.8 (74/5)	14 (70/5)	15 (75/5)	14 (70/5)	99.9 (73/74)	95.7 (67/70)	94.7 (71/75)	95.7 (67/70)
9	100 (5/5)	100 (5/5)	100 (5/5)	100 (5/5)	13.4 (67/5)	10.8 (54/5)	12.2 (61/5)	13.4 (67/5)	97.0 (65/67)	98.1(53/54)	95.1 (58/61)	97.0 (65/67)
10	100 (5/5)	100 (5/5)	100 (5/5)	100 (5/5)	14.4 (72/5)	11.2 (56/5)	13.4 (67/5)	13.4 (67/5)	95.6 (66/69)	87.5 (49/56)	97.0 (65/67)	98.5 (66/67)

* Significance was determined at $p < 0.05$ by the chi-square test.
** Significance was determined at $p < 0.01$ by the chi-square test.
*** Significance was determined at $p < 0.001$ by the chi-square test.

(in silico database for lipids). The number of significant metabolic features ($FDR_{B\text{-}H} < 0.05$) is shown in Table S5. According to metabolomics and lipidomics, 192 and 96 perturbed metabolic and lipidomic features, respectively, were observed in rats exposed to 100 mg B/kg/day. The numbers of significantly up-regulated and down-regulated features among the exposure groups are listed in Table S5. The changes in these metabolic features are shown in Figs. S3 and Tables S6 and S7.

3.7. Perturbation in metabolic pathways

The pathway enrichment analyses suggested that B exposure mainly disrupted the metabolisms of lipids and amino acids (Fig. 3C). Five pathways were associated with significantly upregulated ($p < 0.05$) metabolic features, namely the metabolisms of linoleic acid (LA), thiamine, taurine and hypotaurine, nicotinate and nicotinamide, and glycerophospholipid, and six pathways were associated with significantly downregulated ($p < 0.05$) metabolic features, namely the metabolisms of LA, sphingolipid and α-linolenic acid (α-LA) and biosynthesis of unsaturated fatty acids (FAs), glycerolipid, and FAs. The chemical similarity enrichment analysis demonstrated that some clusters were significantly disturbed in rats exposed to 100 mg B/kg/day ($p < 0.05$), including unsaturated and saturated FAs, unsaturated phosphatidylcholine, dipeptides, ceramides (Cer), triglycerides (TGs), phosphatidylethanolamines, sphingomyelins (SMs), hydroxyeicosatetraenoic acid

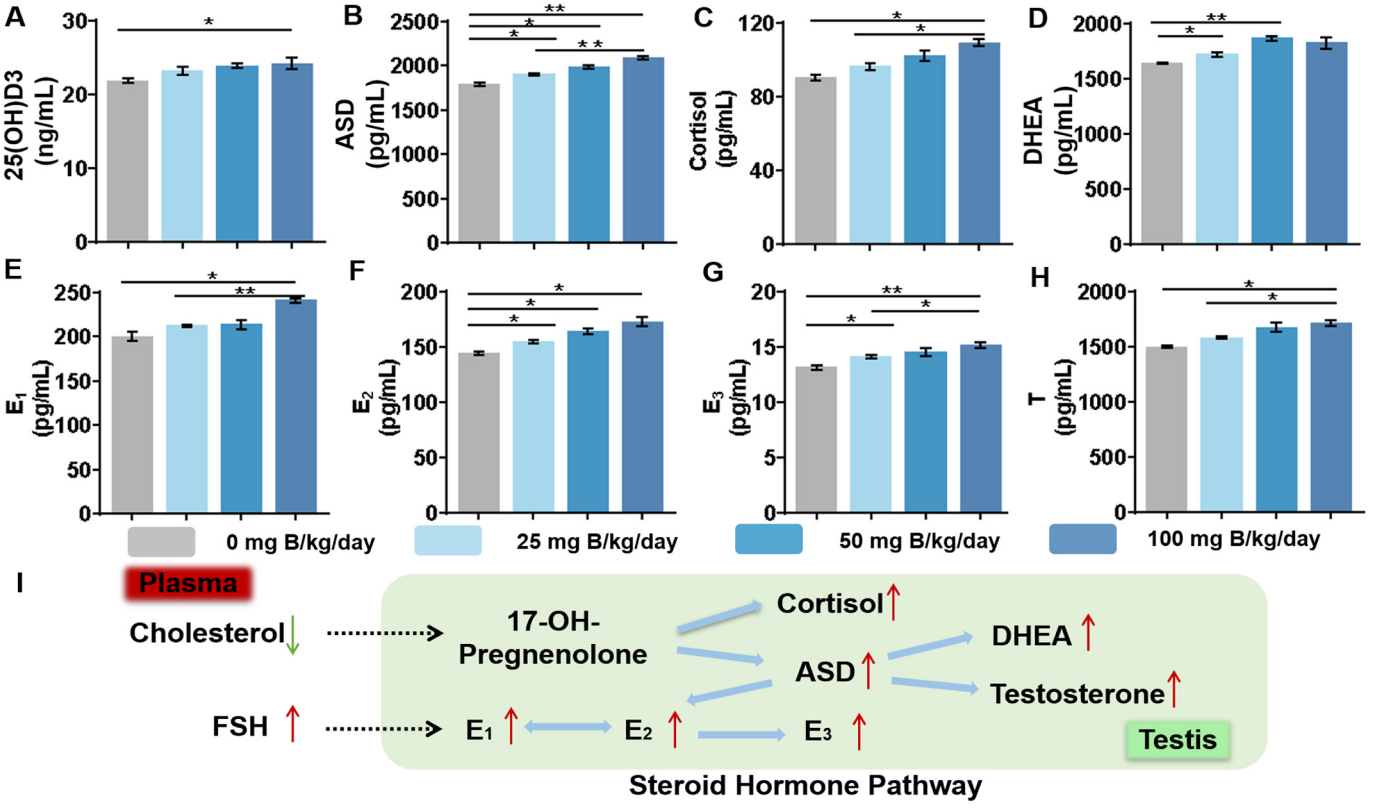

Fig. 2. Concentrations of testicular 25-hydroxyvitamin D_3 (25[OH]D_3)(A), androstenedione (ASD) (B), cortisol (C), dehydroepiandrosterone (DHEA) (D), oestrone (E_1) (E), oestradiol (E_2) (F), oestriol (E_3) (G), and testosterone (T) (H) in male rats exposed to 0, 25, 50 and 100 mg B/kg/day for 28 days. Different colours indicate the samples ($n = 4$) are from different groups. Data are presented as the mean and illustrations of the changes in the steroid hormones in the plasma and testes.

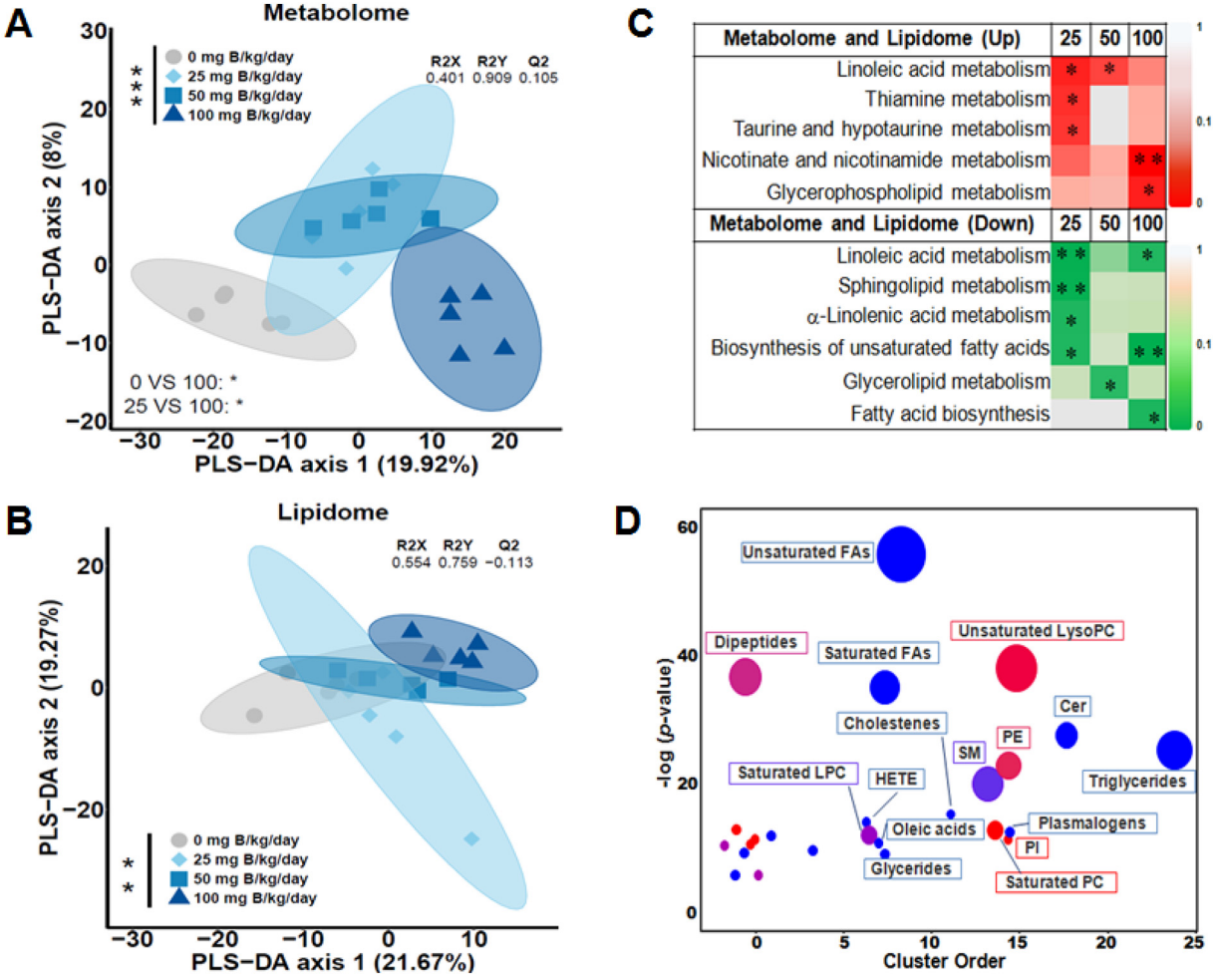

Fig. 3. Partial least squares discriminant analysis (PLS-DA) of plasma untargeted metabolomics (A) and lipidomics (B) results of male rats exposed to 0, 25, 50 and 100 mg B/kg/day for 28 days ($n = 5$). Each point corresponds to a sample, and ovals represent the 95% confidence ellipse around group centroids. Different exposure groups are indicated by different colours. A permutational multivariate analysis of variance test (PERMANOVA, $n = 9999$) indicated that the global metabolic/lipidic profiles were significantly different among the exposure groups. (C) Pathway analysis of the significantly changed metabolites in the plasma metabolome and lipidome conducted by MetaboAnalyst. Cell shading reflects the level of statistical significance of each metabolic pathway associated with boron exposure. The colour bar indicates the level of significance [p; the darker the red (upregulation) or green (downregulation) colour, the greater the significance; grey indicates $p > 0.05$), which is marked by black asterisks: $^{*}p < 0.05$ and $^{**}p < 0.01$. (D) ChemRICH enrichment plot indicating the metabolite clusters affected by exposure to 100 mg B/kg/day. The plot y-axis shows the most significantly altered clusters that were generated by chemical similarity and ontology mapping on the top. The node colour shows the proportion of increased (red) or decreased (blue) metabolites. The chemical enrichment statistics were calculated using the Kolmogorov-Smirnov test. Only significantly different enrichment clusters are shown ($p < 0.05$). Abbreviations: HETE: hydroxyeicosatetraenoic acid; FAs: fatty acids; PE: phosphatidylethanolamines; SM: sphingomyelins; Cer: ceramides; LysoPC: lysophosphatidylcholine; LPC: lysophospholipids; PC: phosphatidylcholines.

(HETE), pyridines and plasmalogens (Fig. 3D). These pathways were predominantly associated with anti- or pro-inflammation, antioxidation defence, energy utilisation, and lipid abnormalities (Fig. 5).

3.8. Associations between metabolic pathways and cytokines, hormones, and enzymes

Orthogonal OPLS-DA modelling further explored the relationships between the disturbed metabolic pathways and the concentrations of IL-5, FSH, G3PDH, MDH, and SDH (Fig. 6). Among them, 14, 15, 15, 7, and 18 pathways with variable influence on projection (VIP) > 1 exhibited positive centred and scaled coefficient (CoeffCS) values, thereby indicating that they were significantly and positively correlated with the concentrations of IL-5, FSH, G3PDH, MDH, and SDH, respectively, whereas 11, 13, 9, 23, and 7 pathways with VIP > 1 exhibited significantly negative correlations with the respective components. For example, diacylglycerol (DG), TGs, and SMs were significantly and positively correlated with IL-5 and G3PDH, but decarboxylated FAs, glycerol, and long-chain FAs were negatively correlated with IL-5 and MDH. Plasmalogen was significantly and positively correlated with IL-5 and G3PDH.

The metabolic pathways were also associated with increases in steroid hormones concentrations (Fig. 6). Among them, 5, 7, 11, 7, 8, 7 and 9 pathways with VIP > 1 exhibited positive CoeffCS values, thereby indicating that they were significantly positively correlated with the concentrations of ASD, cortisol, DHEA, E_1, E_2, E_3 and T, respectively, whereas 23, 25, 17, 23, 25, 24 and 24 pathways with VIP > 1 exhibited significantly negative correlations with the respective components. For example, SAM, arginine and nicotinate were significantly and positively correlated with cortisol, E_1, E_2, E_3, and T, but corticosteroids, endocannabinoid, Mo-hydroxylated FAs, glycerol, and medium- chain FAs were negatively correlated with cortisol, E_1, E_2, E_3 and T.

4. Discussion

Metabolomics of body fluids can provide a synoptic assessment of the systematic metabolic states of organisms. Thus, exploration of global metabolite perturbations in plasma can provide insights into the

mechanisms of B toxicity. To the best of our knowledge, this is the first study to systematically explore the potential mechanisms underlying the effects of B on male reproductive in a comprehensive manner by combining untargeted metabolomics and lipidomics.

4.1. Internal B concentrations in rats after exposure and health risks of B toxicity in humans

Boron is readily absorbed through the gastrointestinal tract (GI), and borax and inorganic borates existing primarily as undissociated boric acid in plasma of mammals cannot be metabolised easily in humans and animals after oral intake because of the large amount of energy required to break the B—O bond (U.S. EPA, 2008a). In our study, the mean B concentration of 422.4 μg/L in plasma obtained after 28 days of exposure of rats to the highest B dose of 100 mg B/kg/day induced the most significant changes in testicular enzymes, hormones, and metabolomics perturbations, compared with the control group. This plasma B concentrations in the rats were comparable to the blood B concentrations in Argentinian mothers (130 μg/L; range: 0.730–610 μg/L) (Igra et al., 2016) and some workers with occupational exposure in the USA (260 μg/L; up to 330 μg/L) (Culver et al., 1994), China (500 μg/L; range: 20.0–3600 μg/L) (Robbins et al., 2010; Scialli et al., 2010) and Turkey (550 μg/L; range: 400–2000 μg/L) (Duydu et al., 2019), indicating our findings might be translated to human effects. However, some extreme occupational and chronic exposures in worker at Turkey showed no signs of adverse reproductive effects (e.g., effects on semen morphology and/or T levels in workers) (Başaran et al., 2020; Bolt et al., 2012; Bolt et al., 2020; Duydu et al., 2011; Duydu et al., 2012a; Duydu et al., 2012b; Duydu et al., 2018a; Duydu et al., 2018b; Robbins et al., 2010), suggesting their exposure doses were substantially lower than those associated with adverse effects in experimental mammals. Notably, our study tested the effects of only short-term exposure; therefore, it is possible that B would be easily bioaccumulated in the body after continuous administration. Moreover, borax kinetics were not considered in this study, which may affect the accurate translation of the effects in rats to humans. Further toxicokinetic studies are needed to accurately extrapolate the effects to humans.

4.2. Boron exposure induced male reproductive toxicity and altered testicular enzyme levels

Exposure to B for 28 days had no effect on the epididymis weight or histopathology. This result is inconsistent with previous studies that showed significant decreases in the epididymis weight after 30 days of exposure to 50 and 100 mg B/kg/day and in both the testis and epididymis weights after 60 days of exposure to the same doses (Dixon et al., 1979; Weir and Fisher, 1972). Although existing data indicate that long-term (>14 weeks) B exposure can cause spermiation inhibition, germ cell loss, morphological changes in epididymal sperm and testicular atrophy (Fail et al., 1991; NTP, 1987; Price et al., 1996a; Price et al., 1996b; Seal and Weeth, 1980; Weir and Fisher, 1972), a recent study did not show significant changes in these parameters after short-term B exposure (< 4 weeks) in (Aktas et al., 2020). Similarly, in this study, male rat fertility, testis histopathology, and the epididymis and seminiferous tubules after 28 days of B exposure showed no clear differences compared with the control group. Our negative findings might be due to the relative short exposure period, different treatment method and/or individual differences in animals.

The significant decrease in live rat foetus rates observed in our study confirmed the previous reports that male fertility is a sensitive endpoint of B-induced reproductive toxicity in animals (Price et al., 1996a; Price et al., 1996b; Seal and Weeth, 1980; Weir and Fisher, 1972). The testes are a major target organ of B toxicity in rats, mice, and dogs (Dixon et al., 1979), and changes in testicular enzymes have been used as biomarkers of B-induced reproductive toxicity. SDH activity has a close correlation with testis weight (Mills and Means, 1972), whereas G3PDH and MDH activities are related to the transformation of spermatocytes to spermatids (Dixon et al., 1979). The increases in G3PDH and MDH activities in our study are consistent with the results of a previous study after exposure of male rates to 25, 50 and 100 mg B/kg/day (Dixon et al., 1979). Their increases reflected a depletion of more differentiated cells, i.e. the disappearance of both spermiogenic cells and premeiotic spermatocytes, and an increase in spermatogonia (Dixon et al., 1979).

4.3. Boron exposure altered steroid hormone and inflammatory cytokine levels

In the testis, FSH stimulated the production of sperm cells in the seminiferous tubules and an essential regulator of sperm maturation. It thus plays an indispensable role in maintaining spermatogenesis (Caroppo and Colpi, 2021; Oduwole et al., 2018a; Oduwole et al., 2018b; Simoni et al., 2020). In a previous study, male rats exposed to 25, 50 and 100 mg B/kg/day via the diet for 30 days and 60 days showed significantly elevated plasma FSH concentrations with a dose-response relationship, but no change in LH concentrations (Dixon et al., 1979). This is similar to our hormone findings of FSH and LH in the plasma of rats exposed to B at different doses. According to the findings of previous and our current studies, even though the concentrations of B did not change in the testes after 28 or 30-day borax exposures, testicular hormones were significantly altered after short-term exposure, suggesting hormone responses were more sensitive than B bioaccumulation upon a short-term exposure. The increase in FSH concentration might help to reduce the damage caused by B exposure to the reproductive system by increasing the number of spermatogonia and spermatocytes. Our findings of an increase in the plasma FSH concentration without a change in the LH concentration in rats are also consistent with previous findings in Turkish workers exposed occupationally to B (Duydu et al., 2011). These results indicate the potential use of FSH, rather than LH, as a sensitive biomarker of B-induced reproductive toxicity.

Boron can increase the release of steroid hormones (Abdelnour et al., 2018; Khaliq et al., 2018). Significantly increases in serum E_2 and T concentrations were observed in both men and post-menopausal women after several weeks of dietary B consumption (Bello et al., 2018; Naghii et al., 2011; Nielsen, 2017). Similarly, in our study, E_1, E_2, E_3, T, cortisol, DHEA, ASD, and ALD were significantly upregulated in the testes of rats exposed to 100 mg B/kg/day, which suggests that B disturbed the metabolic pathway of steroid hormones. The observed increase in FSH could promote E_1 synthesis, thereby contributing to the increased concentrations of downstream E_2 and E_3. The induction of ASD could also upregulate the secretion of E_1, DHEA and T. Although we did not determine the testicular level of 17-OH-pregnenolone, its downstream product cortisol was significantly elevated. Altogether, the elevated plasma FSH concentration significantly increased the concentrations of ASD, E_1, E_2, E_3, and T in the rat testes, thereby confirming that the regulation of steroid hormones synthesis in the testes mainly occurs via the FSH pathway.

Boron can alter inflammatory cytokines. For example, supplementation with 48 and 96 mg B/kg/day significantly reduced the concentrations of IL-2 and IL-4 after 60 days of exposure in rats. IL-5 was reduced in a dose-dependent manner after B exposure (Jin et al., 2017a; Jin et al., 2017b). Thus, B might inhibit the proliferation and differentiation of eosinophils, thereby resulting in a compromised immune system. VEGF can induce vascular proliferation, increase vascular permeability, and change the extracellular matrices under hypoxic conditions, thereby facilitating blood vessel growth (Janani et al., 2021). Exposure to 50 mg B/kg/day significantly promoted VEGF secretion in our male rats, which is consistent with the results of a previous study (Dzondo-Gadet et al., 2002). However, the higher dose of 100 mg B/kg/day did not alter VEGF secretion; thus, further research is needed to confirm and explain this difference.

4.4. Metabolic perturbations relevant to B-induced reproductive toxicity

4.4.1. Reduction in LA and α-LA metabolisms

In our metabolomic and lipidomic analyses, lower concentrations of almost every plasma lipid class were observed after B exposure, particularly 100 mg B/kg/day. Omega-3 (n-3) and omega-6 (n-6) FAs are major groups of essential polyunsaturated FAs (PUFAs) that play important roles in cell membrane structure, fluidity, and signalling (Bjørklund et al., 2020). PUFAs were negatively correlated with IL-5 and MDH, suggesting that lower amounts of PUFAs are associated with inflammation and adversely affect reproductive fitness (Fig. 6). The most abundant dietary PUFAs are LA (18:2, n-6 family) and α-LA (18:3, n-3 family). Because LA plays a vital physiological role in testicular function (Abdelatty et al., 2020), the lower amount of LA indicated that it might be involved in the toxic effects of B. LA can be converted into the important and potent bioactive arachidonic acid (AA; 20:4, n-6 family). Besides acting as a membrane component and providing energy storage, AA regulates steroidogenesis in Leydig cells (Wang et al., 2006). In this study, the AA concentration significantly decreased, which in turn might have caused steroidogenic abnormalities.

4.4.2. Imbalance in oxidant/antioxidant equilibrium

Because oxidative stress can induce peroxidation of lipids in membranes and damage DNA in the testes, the disturbed oxidant/antioxidant equilibrium is a major mechanism of reproductive toxicity (Wang et al., 2020). Similar to other studies, changes in the lipid peroxidation products of the LA, α-LA and oleic acid (C18:1, n-9 family) pathways were observed in our study, which indicated altered oxidative states (Baraldi et al., 2014; Shearer and Newman, 2008). Plasmalogens are the most common ether lipids and have antioxidative properties (Reiss et al., 1997). Significantly lower concentrations of plasmalogens, such as 1-(1-enyl-palmitoyl)-2-palmitoyl-GPC (P-16:0/16:0) and 1-(1-enyl-palmitoyl)-2-arachidonoyl-GPC (P-16:0/20:4)] (Fig. 5 and Tables S6), suggest less protection against oxidative stress. The highest dose of B also resulted in higher concentrations of pyridoxal (vitamin B6) and biopterin compared with the control group, which subsequently affected the methionine/folate cycle (Fig. 5), including cysteine accretion and perturbed antioxidant-related tryptophan metabolism. Therefore, the observed oxidant/antioxidant imbalance may hamper the antioxidative function of important organs, such as the testes, after B exposure.

4.4.3. Changes in energy metabolism

Energy metabolism is crucial to all life activities. Insufficient energy supply caused by triptolide treatment leads to testicular dysfunction and infertility in male mice (Ma et al., 2015). Therefore, abnormal energy metabolism might be another pathway involved in B exposure-induced reproductive toxicity. Significantly lower amounts of medium- and long-chain FAs; PUFAs, including hydroxy and decarboxylated FAs; membrane lipid classes, such as phospholipids (e.g. PE), lysolipids (e.g. lysophosphatidylethanolamine), sphingolipids (i.e. Serine-Cer-HexCer-SM), and lysoplasmalogens (Figs. 4 and 5); and glycerolipids [e.g. DG (Fig. 4A), TG (Fig. 4H) and glycerol (a biomarker of lipolysis)] are indicators of lower lipids utilisation with a lower output of useable energy. Significantly less circulating carnitine-conjugated FAs [e.g., acyl-carnitine palmitoleoylcarnitine (C16:1) and dihomo-linoleoylcarnitine (C20:2)] were found at 100 mg B/kg/day (Table S6). The conjugation of FAs with carnitine is primarily involved in the transport across mitochondrial membranes and subsequent β-oxidation to achieve balanced energy homeostasis. Therefore, it can be postulated that longer-chain acylcarnitine congeners are sensitive to B and thus result in less β-oxidation and lower supplies of energy from the mitochondria.

Lower concentrations of α-ketoglutarate indicate suppression of the tricarboxylic acid (TCA) cycle, which is an important energy metabolism pathway involving the final oxidation of proteins, amino acids, fats, and carbohydrates for energy supply (Xiao et al., 2016). We found a significant increase in creatine metabolism, a biomarker of muscle metabolism, which was positively correlated with FSH, G3PDH, and MDH at 100 mg B/kg/day (Figs. 5 and 6 and Table S6). Depletion of the substrate

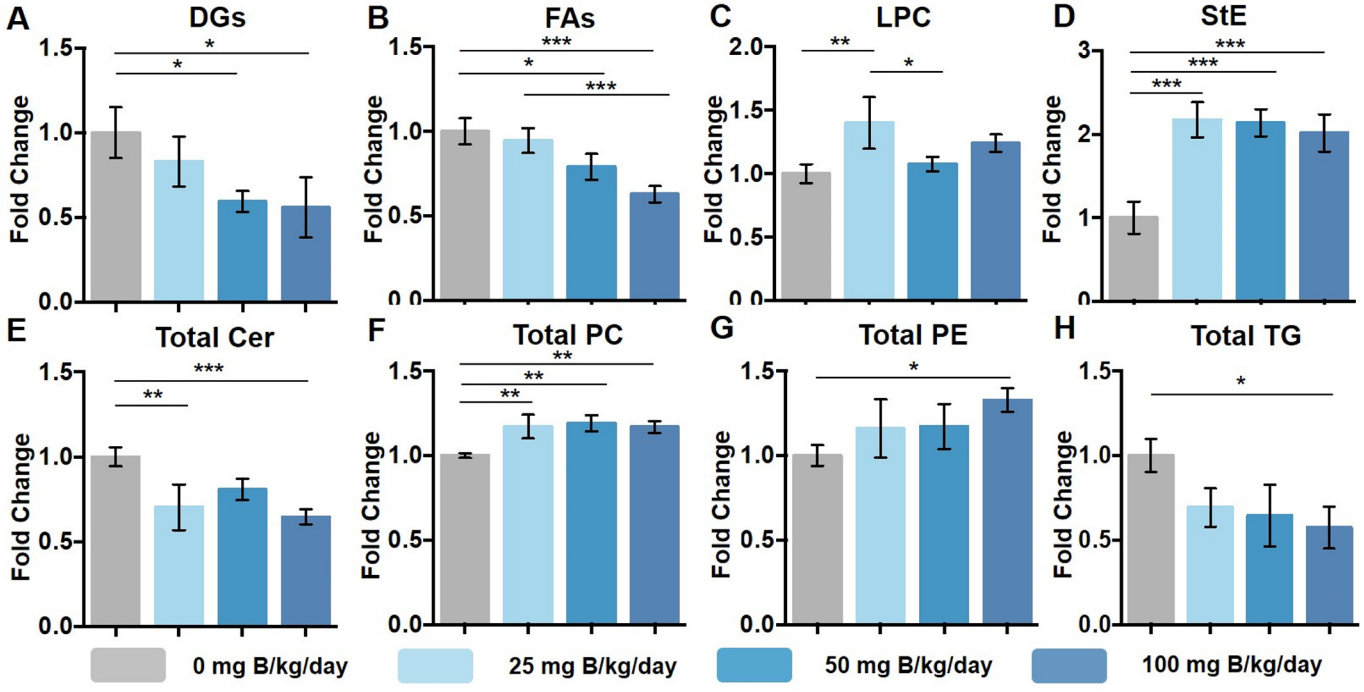

Fig. 4. Fold changes in major plasma lipid classes (A–H) in male rats exposed to 0, 25, 50 and 100 mg B/kg/day for 28 days. Different colours indicate that the samples ($n = 5$) are from different groups. Data are presented as the mean and standard error of the mean. Significance was determined at $p < 0.05^{*}$, $p < 0.01^{**}$ and $p < 0.001^{***}$ using Student's *t*-test. Abbreviations: diacylglycerol (DG), fatty acids (FA), lysophospholipids (LPC), steroids (StE), ceramides (Cer), phosphatidylcholines (PC), phosphatidylethanolamines (PE) and triacylglycerol (TG).

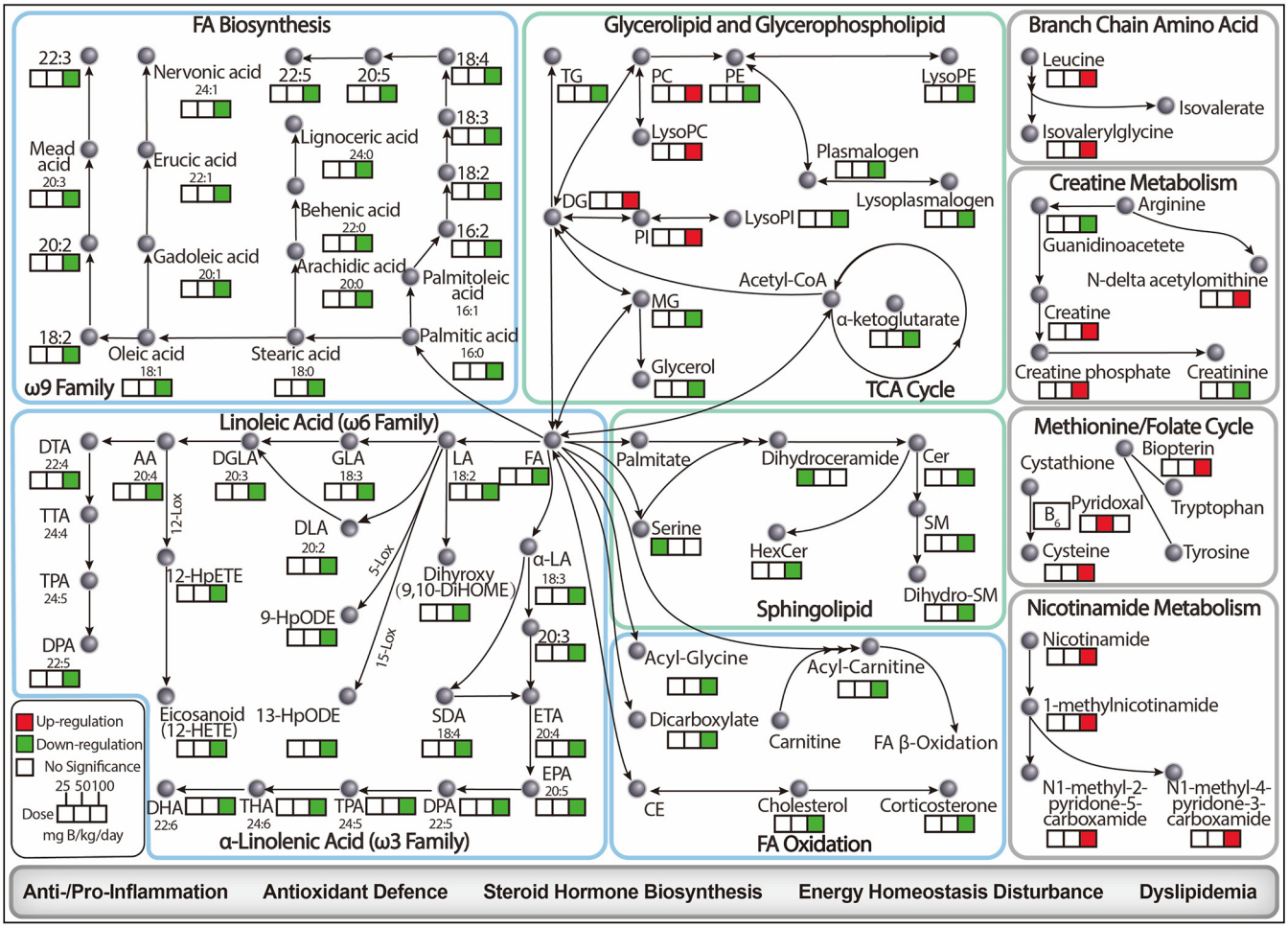

Fig. 5. Putative mechanism underlying boron exposure-induced reproductive toxicity indicated by untargeted metabolomics and lipidomics. After administration, boron can enter the blood and lead to inhibition of inflammatory responses, antioxidant imbalance, perturbation of steroid hormone biosynthesis, abnormal energy homeostasis and dyslipidemia, which ultimately result in reproductive toxicity. Significantly changed metabolites during exposure are labeled with different colours (red: upregulation; green: downregulation; red/green: upregulation or downregulation; grey: not changed). Each detected change in the related metabolic pathway is shown in Tables S5 and S6. Abbreviations: arachidonic acid (AA), cholesteryl ester (CE), Ceramides (Cer), diacylglycerol (DG), dihomo γ-linolenic acid (DGLA), docosahexaenoic acid (DHA), 9,10-dihydroxy-12-octadecenoic acid (9,10-DiHOME), Dihomo linolenic acid (DLA), docosapentaenoic acid (DPA), docosatetraenoic acid (DTA), eicosapentaenoic acid (EPA), eicosatetraenoic acid (ETA), fatty acids (FA), ganglioside (GM), hexaceramides (HexCer), 12-hydroxyeicosatetraenoic acid (12-HETE), 9-hydroxyoctadecadienoic acid (9-HODE), lysophosphatidic acid (LysoPA), lyso-phosphatidylcholine (LysoPC), lyso-Phosphatidylethanolamine (LysoPE), lysophosphatidylinositol (LysoPI), linolenic acid (LA), γ-linolenic acid (GLA), monoglyceride (MG), oxidized sphingomyelin (Oxidized SM), phosphatidic acid (PA), phosphatidylcholine (PC), phosphatidylethanolamine (PE), phosphatidylinositol (PI), phosphatidylserine (PS), stearidonic acid (SDA), sphingomyelin (SM), total cholesterol (TCHOL), triacylglycerol (TG), tetracosahexaenoic acid (THA), tetracosapentaenoic acid (TPA) and tetracosatetraenoic acid (TTA).

creatinine with the corresponding accumulation of high-energy molecules, creatine phosphate and creatine indicated that arginine metabolism could be directed to promote creatine production to support muscle metabolism. The downstream catabolite N-delta-acetylornithine might represent shunting of excess arginine owing to creatine utilisation. These results indicate that B exposure might shift energy utilisation from lipid burning to muscle metabolism, while reducing/managing oxidative stress and inflammation.

Consistent with increased creatine production and putative muscle metabolism, significantly elevated branched-chain amino acids (BCAAs) of leucine and their corresponding *N*-acetyl derivatives, were found at 100 mg B/kg/day (Fig. 5 and Table S6). As the most abundant essential amino acids, BCAAs are not only substrates for nitrogenous compound synthesis, but also signalling molecules that regulate glucose metabolism, lipid and protein synthesis and immunity. Boron exposure caused a significant depletion of 3-hydroxy-2-ethylpropion-ate (Korman et al., 2005), which was consistent with B increasing lipid utilisation, but increased the catabolism of skeletal muscle for energy production. The changes in nicotinamide (vitamin B3) metabolism also indicate that B altered the energy homeostasis (Fig. 5). The highest dose of B led to significant increases in nicotinamide and nicotinamide-derived metabolites (e. g., 1-methylnicotinamide and N1-methyl-2-pyridone-5-carboxyamide). Nicotinamide is a key intermediate in nicotinamide adenine dinucleotide (NAD) synthesis, which play a critical role in energy metabolism. Higher nicotinamide levels might be linked to increased turnover of NAD for adenosine diphosphate (ADP) ribosylation.

4.4.4. Perturbation of steroid hormones synthesis

Sex steroid hormones are essential for the development of gonads and secondary sexual characteristics and for the maintenance of male reproduction. Hormones are often regulated by upstream precursors and activities of steroidogenic enzymes. Although B did not alter the plasma level of LH, those of cholesterol, beta-sitosterol, and campesterol were significantly decreased. The plasma level of cholesterol, an important steroid precursor molecule, was 0.66 times lower in the

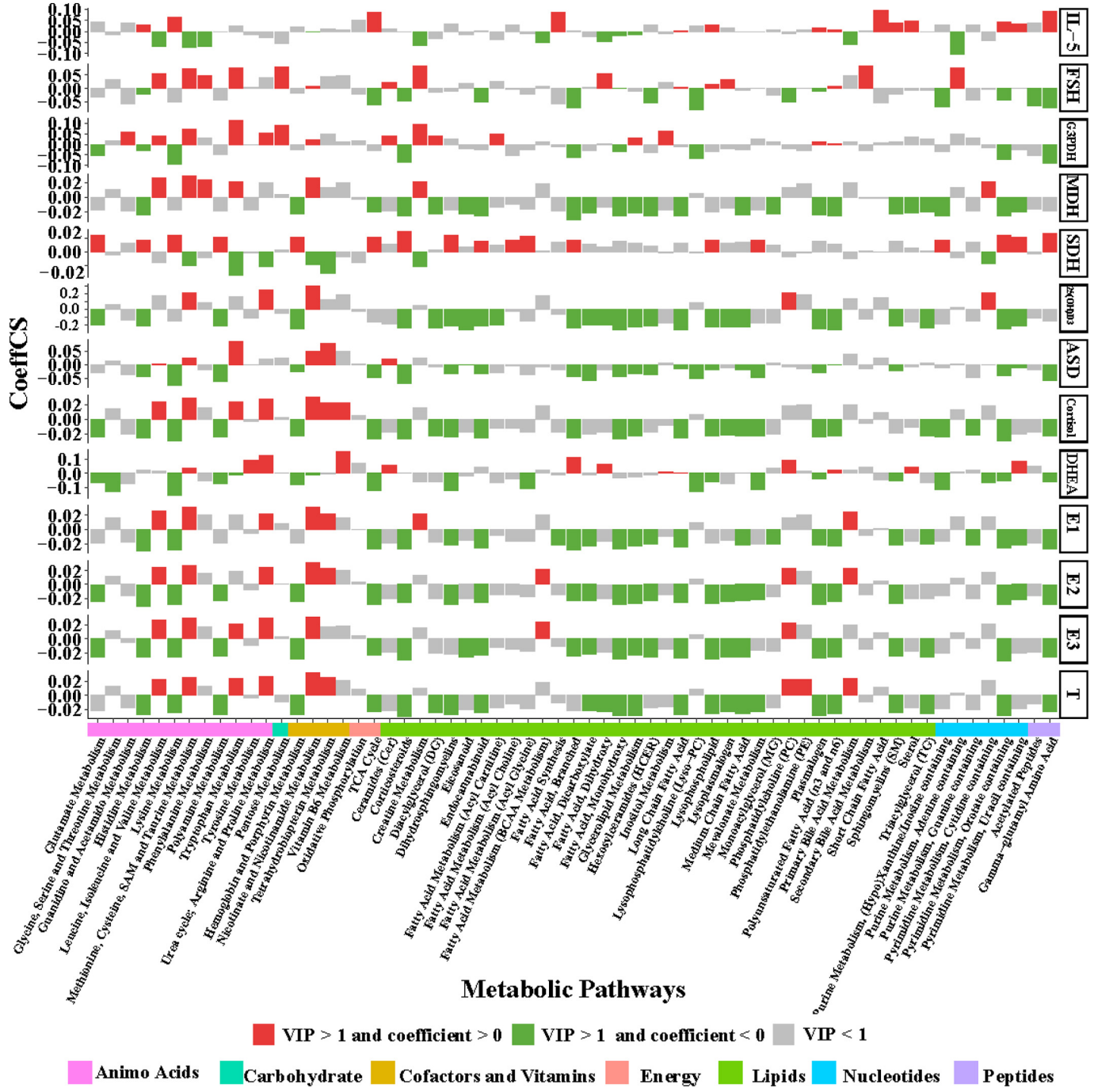

Fig. 6. Coefficients of centered and scaled *X* data (metabolic pathways; CoeffCS) with the metabolic levels as *X* variables and levels of inflammatory cytokine interleukin-5 (IL-5), testicular enzymes of glyceraldehyde-3-phosphate dehydrogenase (G3PDH), malate dehydrogenase (MDH) and sorbitol dehydrogenase (SDH), gonadotropin follicle-stimulating hormone (FSH), testicular 25-hydroxyvitamin D_3 (25[OH]D_3), androstenedione (ASD), cortisol, dehydroepiandrosterone (DHEA), oestrone (E_1), oestradiol (E_2), oestriol (E_3), and testosterone (T) as *Y* variables using orthogonal partial least squares discriminant analysis. The metabolic pathways labeled with red, green and grey represent those with a variable influence on projection (VIP) >1 and coefficient > 0, VIP > 1 and coefficient < 0, and VIP < 1, respectively. Red and green metabolic pathways suggest significant positive and negative contributions to the inflammatory cytokines, testicular enzymes, gonadotropin and hormones, respectively.

100 mg B/kg/day group than in the control group, indicating that B exposure induced the conversion of cholesterol to downstream steroid hormones (e.g., cortisol, ASD and DHEA).

4.4.5. Pathways relevant to inflammatory responses

AA can be metabolised via cyclooxygenase and lipoxygenase enzymes into a large family of eicosanoid products, which play important roles in the initiation and maintenance of inflammation. Significantly lower levels of eicosanoid products of polyunsaturated hydroxy FAs at 100 mg B mg/kg/day (12-HETE; Fig. 5) suggested that lipid peroxidation derivatives are involved in B exposure-induced inflammation. In addition, n-3 long-chain PUFAs [eicosapentaenoic acid (EPA) and docosahexaenoic acid (DHA)] can be synthesised from α-LA. The derivatives of EPA and DHA have potent anti-inflammatory properties and play important roles in orchestrating immunity and inflammation (Allaire et al., 2016; Ohue-Kitano et al., 2018; Zárate et al., 2017). α-LA

and its oxidized products can regulate many activities via nuclear receptors, thereby modulating immune responses (Rousseau et al., 2016). Oleic acid is the primary representative of monounsaturated FAs and can reduce lipids synthesis and attenuate inflammation and oxidative status. In this study, significant decreases observed in the levels of EPA, DHA, oleic acid and their derivatives at 100 mg B/kg/day (Fig. 5 and Table S6) provide evidence of the involvement of inflammation in the effects of B toxicity. The metabolomics and lipidomics data (e.g. lysine metabolism, TCA cycle and FA and short-chain FA synthesis) are consistent with the decrease in the IL-5 level at 100 mg B/kg/day (Fig. 6), which confirms the occurrence of perturbed inflammatory responses.

5. Conclusions

Boron exposure via oral gavage for 28 days caused significant adverse effects on the reproductive fitness of male rats, as evidenced by the increasing foetal malformations and changes in the testicular enzymes of MDH, SDH, G3PDH and plasma FSH of rats exposed to the highest B dose of 100 mg/kg/day. Steroid hormones in the testes were significantly elevated, which disrupted reproductive functions. Combined metabolomics and lipidomics illustrated that exposure to 100 mg B/kg/day reduced the plasma lipid concentrations, FA biosynthesis and metabolism, β-oxidation, TG synthesis and glycerophospholipids and TCA intermediate concentrations, suggesting that high B exposure caused changes in inflammatory responses, antioxidation responses, energy utilisation and steroid hormone synthesis. This was possibly compensated for by increased skeletal muscle metabolism, as indicated by the increased amino acid metabolism, creatine production, BCAA metabolism and nicotinamide availability. The correlations between the disturbances in energy metabolism, inflammatory responses, oxidative stress and functional endpoints of reproduction may be helpful in elucidating the mechanisms of B-induced reproductive toxicity. Because B removal is of significance in RO treatment plants, the findings of this study suggest the need for a comprehensive evaluation of the principal health risks related to drinking desalinated water.

CRediT authorship contribution statement

Chong Wang: Investigation, Conceptualization, Formal analysis, Writing – original draft, Data curation, Visualization, Writing - review & editing. **Ziqing Kong:** Data curation, Visualization. **Lian Duan:** Funding acquisition, Investigation, Conceptualization. **Fuchang Deng:** Data curation. **Yuanyuan Chen:** Data curation. **Sheng Quan:** Data curation. **Xiaohui Liu:** Data curation. **Yu'e Cha:** Visualization. **Yufeng Gong:** Writing – review & editing. **Chao Wang:** Investigation, Conceptualization. **Ying Shi:** Investigation, Conceptualization. **Wen Gu:** Investigation, Conceptualization. **Yuanzheng Fu:** Visualization. **Donghai Liang:** Visualization. **John P. Giesy:** Writing - review & editing. **Hongwei Zhang:** Investigation, Conceptualization. **Song Tang:** Funding acquisition, Project administration, Supervision, Writing – review & editing.

Declaration of competing interest

The authors declare no conflict of interest.

Acknowledgements

This study was funded by the Research of Short-Term Exposure Risk and Emergency Control Technology in Emergency Event Water Supply of the National Science and Technology Major Project of China Grant No. 2015ZX07402002 to Dr. Zhang, the National Natural Science Foundation of China Grant No. 21806157 to Dr. Duan, and the Young Scholar Scientific Research Foundation Grant No. 2018A201 from the China CDC and Start-Up Funding from the NIEH, China CDC to Dr. Tang.

Appendix A. Supplementary data

Supplementary data to this article can be found online at https://doi.org/10.1016/j.scitotenv.2021.147370.

References

Abdelatty, A.M., Badr, O.A.M., Mohamed, S.A., Khattab, M.S., Dessouki, S.M., Farid, O.A.A., Elolimy, A.A.S., Sakr, O.G., Elhady, M.A., Mehesen, G., Bionaz, M., 2020. Long term conjugated linoleic acid supplementation modestly improved growth performance but induced testicular tissue apoptosis and reduced sperm quality in male rabbit. PLoS One 15, e0226070. https://doi.org/10.1371/journal.pone.0226070.

Abdelnour, S.A., Abd El-Hack, M.E., Swelum, A.A., Perillo, A., Losacco, C., 2018. The vital roles of boron in animal health and production: a comprehensive review. J. Trace Elem. Med. Biol. 50, 296–304. https://doi.org/10.1016/j.jtemb.2018.07.018.

Aktas, S., Kum, C., Aksoy, M., 2020. Effects of boric acid feeding on the oxidative stress parameters in testes, sperm parameters and DNA damage in mice. J. Trace Elem. Med. Biol. 58, 126447. https://doi.org/10.1016/j.jtemb.2019.126447.

Allaire, J., Couture, P., Leclerc, M., Charest, A., Marin, J., Lépine, M.C., Talbot, D., Tchernof, A., Lamarche, B., 2016. A randomized, crossover, head-to-head comparison of eicosapentaenoic acid and docosahexaenoic acid supplementation to reduce inflammation markers in men and women: the Comparing EPA to DHA (ComparED) Study. Am. J. Clin. Nutr. 104, 280–287. https://doi.org/10.3945/ajcn.116.131896.

Aquatech, 2019. Desalination: Our Essential Guide To Desalination and the Global Water Crisis. https://www.aquatechtrade.com/news/desalination/desalination-essential-guide/.

Baraldi, F., Dalalio, F., Teodoro, B., Prado, I., Curti, C., Alberici, L., 2014. Body energy metabolism and oxidative stress in mice supplemented with conjugated linoleic acid (CLA) associated to oleic acid. Free Radic. Biol. Med. 75 (Suppl., S21-S53). https://doi.org/10.1016/j.freeradbiomed.2014.10.733.

Barupal, D.K., Fiehn, O., 2017. Chemical similarity enrichment analysis (ChemRICH) as alternative to biochemical pathway mapping for metabolomic datasets. Sci. Rep. 7, 14567. https://doi.org/10.1038/s41598-017-15231-w.

Başaran, N., Duydu, Y., Bacanlı, M., Gül Anlar, H., Dİlslz, S.A., Üstündağ, A., Yalçın, C.Ö., Schwerdtle, T., Bolt, H.M., 2020. Evaluation of oxidative stress and immune parameters of boron exposed males and females. Food Chem. Toxicol. 142, 111488. https://doi.org/10.1016/j.fct.2020.111488.

Bello, M., Guadarrama-García, C., Velasco-Silveyra, L.M., Farfán-García, E.D., Soriano-Ursúa, M.A., 2018. Several effects of boron are induced by uncoupling steroid hormones from their transporters in blood. Med. Hypotheses 118, 78–83 doi:118. https://doi.org/10.1016/j.mehy.2018.06.024.

Bjørklund, G., Dadar, M., Doşa, M.D., Chirumbolo, S., Pen, J.J., 2020. Insights on dietary omega-6/omega-3 polyunsaturated fatty acid (PUFA) ratio in oxidative metabolic pathways of oncological bone disease and global health. Curr. Med. Chem. https://doi.org/10.2174/0929867327666200427095331.

Bolt, H.M., Başaran, N., Duydu, Y., 2020. Effects of boron compounds on human reproduction. Arch. Toxicol. 94, 717–724. https://doi.org/10.1007/s00204-020-02700-x.

Breitner, L.N., Howe, K.J., Minakata, D., 2018. Boron can be used to predict trace organic rejection through reverse osmosis membranes for potable reuse. Environ. Sci. Technol. 52, 13,871–13,878. https://doi.org/10.1021/acs.est.8b03390.

Bundy, J.G., Davey, M.P., Viant, M.R., 2009. Environmental metabolomics: a critical review and future perspectives. Metabolomics. 5, 3–21. https://doi.org/10.1007/s11306-008-0152-0.

Bureau for Chemical Substances, 2013. CLH report for Boric Acid "Proposal for Harmonised Classification and Labelling". Annnex VI, Part 2. https://echa.europa.eu/documents/10162/13626/clh_report_boric_acid_en.pdf.

Caroppo, E., Colpi, G.M., 2021. Hormonal treatment of men with nonobstructive azoospermia: what does the evidence suggest? J. Clin. Med. 103 (3), 387. https://doi.org/10.3390/jcm10030387.

Chong, J., Wishart, D., Xia, J., 2019. Using MetaboAnalyst 4.0 for comprehensive and integrative metabolomics data analysis. Curr. Protoc. Bioinformatics 68, e86. https://doi.org/10.1002/cpbi.86.

Cui, Y., Winton, M., Zhang, Z., Rainey, C., Marshall, J., Dekernion, J., Eckhert, C., 2004. Dietary boron intake and prostate cancer risk. Oncol. Rep. 11, 887–892.

Culver, B.D., Shen, P.T., Taylor, T.H., Lee-Feldstein, A., Anton-Culver, H., Strong, P.L., 1994. The relationship of blood- and urine-boron to boron exposure in borax-workers and usefulness of urine-boron as an exposure marker. Environ. Health Perspect. 102, 133–137. https://doi.org/10.1289/ehp.94102s7133.

Dixon, R.L., Sherins, R.J., Lee, I.P., 1979. Assessment of environmental factors affecting male fertility. Environ. Health Perspect. 30, 53–68. https://doi.org/10.1289/ehp.793053.

Duydu, Y., Başaran, N., Üstündağ, A., Aydin, S., Ündeğer, Ü., Ataman, O.Y., Aydos, K., Düker, Y., Ickstadt, K., Waltrup, B.S., Golka, K., Bolt, H.M., 2011. Reproductive toxicity parameters and biological monitoring in occupationally and environmentally boron-exposed persons in Bandirma, Turkey. Arch. Toxicol. 85, 589–600. https://doi.org/10.1007/s00204-011-0692-3.

Duydu, Y., Basaran, N., Bolt, H.M., 2012a. Exposure assessment of boron in Bandırma boric acid production plant. J. Trace Elem. Med. Biol. 26, 161–164. https://doi.org/10.1016/j.jtemb.2012.03.008.

Duydu, Y., Basaran, N., Ustundag, A., Aydin, S., Undeger, U., Ataman, O.Y., Aydos, K., Duker, Y., Ickstadt, K., Waltrup, B.S., Golka, K., Bolt, H.M., 2012b. Assessment of DNA integrity (COMET assay) in sperm cells of boron-exposed workers. Arch. Toxicol. 86, 27–35. https://doi.org/10.1007/s00204-011-0743-9.

Duydu, Y., Başaran, N., Aydın, S., Üstündağ, A., Yalçın, C.Ö., Anlar, H.G., Bacanlı, M., Aydos, K., Atabekoğlu, C.S., Golka, K., Ickstadt, K., Schwerdtle, T., Werner, M., Meyer, S., Bolt, H.M., 2018a. Evaluation of FSH, LH, testosterone levels and semen parameters in male boron workers under extreme exposure conditions. Arch. Toxicol. 92, 3051–3059. https://doi.org/10.1007/s00204-018-2296-7.

Duydu, Y., Başaran, N., Üstündağ, A., Aydın, S., Yalçın, C.Ö., Anlar, H.G., Bacanlı, M., Aydos, K., Atabekoğlu, C.S., Golka, K., 2018b. Birth weights of newborns and pregnancy outcomes of environmentally boron-exposed females in Turkey. Arch. Toxicol. 92, 2475–2485. https://doi.org/10.1007/s00204-018-2238-4.

Duydu, Y., Başaran, N., Yalçın, C.Ö., Üstündağ, A., Aydın, S., Anlar, H.G., Bacanlı, M., Aydos, K., Atabekoğlu, C.S., Golka, K., Ickstadt, K., Schwerdtle, T., Werner, M., Bolt, H.M., 2019. Boron-exposed male workers in Turkey: no change in sperm Y:X chromosome ratio and in offspring's sex ratio. Arch. Toxicol. 93, 743–751. https://doi.org/10.1007/s00204-019-02391-z.

Dzondo-Gadet, M., Mayap-Nzietchueng, R., Hess, K., Nabet, P., Belleville, F., Dousset, B., 2002. Action of boron at the molecular level: effects on transcription and translation in an acellular system. Biol. Trace Elem. Res. 85, 23–33. https://doi.org/10.1385/BTER:85:1:23.

Fail, P.A., George, J.D., Seely, J.C., Grizzle, T.B., Heindel, J.J., 1991. Reproductive toxicity of boric acid in Swiss (CD-1) mice: assessment using the continuous breeding protocol. Fundam. Appl. Toxicol. 17, 225–239. https://doi.org/10.1016/0272-0590(91)90215-p.

Farfán-García, E.D., Castillo-Mendieta, N.T., Ciprés-Flores, F.J., Padilla-Martínez, I.I., Trujillo-Ferrara, J.G., 2016. Current data regarding the structure-toxicity relationship of boron-containing compounds. Toxicol. Lett. 258, 115–125. https://doi.org/10.1016/j.toxlet.2016.06.018.

Gao, S., Wan, Y., Li, W., Huang, C., 2019. Visualized networking of co-regulated lipids in human blood based on high-throughput screening data: implications for exposure assessment. Environ. Sci. Technol. 53, 2862–2872. https://doi.org/10.1021/acs.est.8b06289.

Goldbach, H.E., Wimmer, M.A., 2007. Boron in plants and animals: is there a role beyond cell-wall structure? J. Plant Nutr. Soil Sci. 170, 39–48. https://doi.org/10.1002/jpln.200625161.

Gu, J., Ji, C., Yue, S., Shu, D., Su, F., Zhang, Y., Xie, Y., Zhang, Y., Liu, W., Zhao, M., 2018. Enantioselective effects of Metalaxyl enantiomers in adolescent rat metabolic profiles using NMR-based metabolomics. Environ. Sci. Technol. 52, 5438–5447. https://doi.org/10.1021/acs.est.7b06540.

Hammes, G.G., Wu, C.-W., 1971. Regulation of enzymatic activity. Science. 172, 1205–1211. https://doi.org/10.1126/science.172.3989.1205.

Han, X., 2016. Lipidomics for studying metabolism. Nat. Rev. Endocrinol. 12, 668–679. https://doi.org/10.1038/nrendo.2016.98.

Howe, P.D., 1998. A review of boron effects in the environment. Biol. Trace Elem. Res. 66, 153–166. https://doi.org/10.1007/bf02783135.

Hu, Q., Li, S., Qiao, E., Tang, Z., Jin, E., Jin, G., Gu, Y., 2014. Effects of boron on structure and antioxidative activities of spleen in rats. Biol. Trace Elem. Res. 158, 73–80. https://doi.org/10.1007/s12011-014-9899-5.

Hunt, C.D., Idso, J.P., 1999. Dietary boron as a physiological regulator of the normal inflammatory response: a review and current research progress. J. Trace Elem. Exp. Med. 12, 221–233. https://doi.org/10.1002/(sici)1520-670x(1999)12:3<221::aid-jtra6>3.0.co;2-x.

Igra, A.M., Harari, F., Lu, Y., Casimiro, E., Vahter, M., 2016. Boron exposure through drinking water during pregnancy and birth size. Environ. Int. 95, 54–60. https://doi.org/10.1016/j.envint.2016.07.017.

Janani, R., Anitha, R.E., Perumal, M.K., Divya, P., Baskaran, V., 2021. Astaxanthin mediated regulation of VEGF through HIF1α and XBP1 signaling pathway: An insight from ARPE-19 cell and streptozotocin mediated diabetic rat model. Exp. Eye Res. https://doi.org/10.1016/j.exer.2021.108555.

Jin, E., Li, S., Ren, M., Hu, Q., Gu, Y., Li, K., 2017a. Boron affects immune function through modulation of splenic T lymphocyte subsets, cytokine secretion, and lymphocyte proliferation and apoptosis in rats. Biol. Trace Elem. Res. 178, 261–275. https://doi.org/10.1007/s12011-017-0932-3.

Jin, E., Ren, M., Liu, W., Liang, S., Hu, Q., Gu, Y., Li, S., 2017b. Effect of boron on thymic cytokine expression, hormone secretion, antioxidant functions, cell proliferation, and apoptosis potential via the extracellular signal-regulated kinases 1 and 2 signaling pathway. J. Agric. Food Chem. 65, 11280–11291. https://doi.org/10.1021/acs.jafc.7b04069.

Kabu, M., Akosman, M.S., 2013. Biological effects of boron. Rev. Environ. Contam. Toxicol. 225, 57–75 New York. https://doi.org/10.1007/978-1-4614-6470-9_2.

Khaliq, H., Zhong, J.M., Peng, K.M., 2018. The physiological role of boron on health. Biol. Trace Elem. Res. 1861 (1), 31–51. https://doi.org/10.1007/s12011-018-1284-3.

Korman, S.H., Andresen, B.S., Zeharia, A., Gutman, A., Boneh, A., Pitt, J.J., 2005. 2-ethylhydracrylic aciduria in short/branched-chain acyl-CoA dehydrogenase deficiency: application to diagnosis and implications for the R-pathway of isoleucine oxidation. Clin. Chem. 51, 610–617. https://doi.org/10.1373/clinchem.2004.043265.

Lee, I.P., Sherins, R.J., Dixon, R.J., 1978. Evidence for induction of germinal aplasia in male rats by environmental exposure to boron. Toxicol. Appl. Pharmacol. 452 (2), 577–590. https://doi.org/10.1016/0041-008x(78)90119-9.

Liang, D.H., Moutinho, J.L., Golan, R., Yu, T.W., Ladva, C.N., Niedzwiecki, M., Walker, D.I., Sarna, S.E., Chang, H.H., Greenwald, R.J.D.P.R., Sarnat, A.G., J., A., 2018. Use of high-resolution metabolomics for the identification of metabolic signals associated with traffic-related air pollution. Environ. Int. 120, 145–154. https://doi.org/10.1016/j.envint.2018.07.044.

Linnder, R.E., Strader, L.F., Rehnberg, G.L., 1990. Effect of acute exposure to boric acid on the male reproductive system of the rat. J. Toxicol. Environ. Health 312 (2), 133–146. https://doi.org/10.1080/15287399009531443.

Ma, B., Qi, H., Li, J., Xu, H., Chi, B., Zhu, J., Yu, L., An, G., Zhang, Q., 2015. Triptolide disrupts fatty acids and peroxisome proliferator-activated receptor (PPAR) levels in male mice testes followed by testicular injury: a GC-MS based metabolomics study. Toxicology. 336, 84–95. https://doi.org/10.1016/j.tox.2015.07.008.

Mills, N.C., Means, A.R., 1972. Sorbitol dehydrogenase of rat testis: changes of activity during development, after hypophysectomy and following gonadotrophic hormone administration. Endocrinology. 91, 147–156. https://doi.org/10.1210/endo-91-1-147.

Miwa, K., Takano, J., Omori, H., Seki, M., Shinozaki, K., Fujiwara, T., 2007. Plants tolerant of high boron levels. Science. 318 (5855), 1417-1417. https://doi.org/10.1126/science.1146634.

Murray, F.J., 1995. A human health risk assessment of boron (boric acid and borax) in drinking water. Regul. Toxicol. Pharmacol. 22, 221–230. https://doi.org/10.1006/rtph.1995.0004.

Naghii, M.R., Mofid, M., Asgari, A.R., Hedayati, M., Daneshpour, M.S., 2011. Comparative effects of daily and weekly boron supplementation on plasma steroid hormones and proinflammatory cytokines. J. Trace Elem. Med. Biol. 25 (1), 54–58. https://doi.org/10.1016/j.jtemb.2010.10.001.

Nan, X.R., Liu, J., Wang, X.L., Pan, X., Wang, H., M, X., Zhang, X., 2018. Preparation of superhydrophilic adsorbents with 3DOM structure by water- soluble colloidal crystal templates for boron removal from natural seawater. ACS Appl. Mater. Interfaces 10 (43), 36,918–36,925. https://doi.org/10.1021/acsami.8b11763.

National Health Commission of the People's Republic of China, 2020. Standards for drinking water quality. GB5749-2006 China. http://std.samr.gov.cn/search/std?q=%20GB5749%EF%BC%8D2006.

Nguyen, A., Rudge, S.A., Zhang, Q., Wakelam, M.J., 2017. Using lipidomics analysis to determine signalling and metabolic changes in cells. Curr. Opin. Biotechnol. 43, 96–103. https://doi.org/10.1016/j.copbio.2016.10.003.

Nielsen, F.H., 1998. The justification for providing dietary guidance for the nutritional intake of boron. Biol. Trace Elem. Res. 66, 319–330. https://doi.org/10.1007/BF02783145.

Nielsen, F.H., 2017. Historical and recent aspects of boron in human and animal health. Bor. Dergisi 2 (3), 153–160 2017.

Nielsen, F.H., Penland, J.G., 1999. Boron supplementation of peri-menopausal women affects boron metabolism and indices associated with macromineral metabolism, hormonal status and immune function. J. Trace Elem. Exp. Med. 12, 251–261. https://doi.org/10.1002/(SICI)1520-670X(1999)12:3<251::AID-JTRA8>3.0.CO;2-I.

NTP, 1987. NTP toxicology and carcinogenesis studies of boric acid (CAS no. 10043-35-3) in B6C3F1 mice (feed studies). Natl. Toxicol. Program. Tech. Rep. Ser. 324, 1–126.

Oduwole, O.O., Peltoketo, H., Huhtaniemi, I.T., 2018a. Role of follicle-stimulating hormone in spermatogenesis. Front. Endocrinol. 9, 763. https://doi.org/10.3389/fendo.2018.00763.

Oduwole, O.O., Peltoketo, H., Poliandri, A., Vengadabady, L., Chrusciel, M., Doroszko, M., Samanta, L., Owen, L., Keevil, B., Rahman, N.A., Huhtaniemi, I.T., 2018b. Constitutively active follicle-stimulating hormone receptor enables androgen-independent spermatogenesis. J. Clin. Invest. 128 (5), 1787–1792. https://doi.org/10.1172/JCI96794.

Ohue-Kitano, R., Yasuoka, Y., Goto, T., Kitamura, N., Park, S.B., Kishino, S., Kimura, I., Kasubuchi, M., Takahashi, H., Li, Y., Yeh, Y., Jheng, H., Iwase, M., Tanaka, M., Masuda, S., Inoue, T., Yamakage, H., Kusakabe, T., Tani, F., Shimatsu, A., Takahashi, N., Ogawa, J., Satoh-Asahara, N., Kawada, T., 2018. α-Linolenic acid-derived metabolites from gut lactic acid bacteria induce differentiation of anti-inflammatory M2 macrophages through G protein-coupled receptor 40. FASEB J. 32, 304–318. https://doi.org/10.1096/fj.201700273R.

Penland, J.G., 1998. The importance of boron nutrition for brain and psychological function. Biol. Trace Elem. Res. 66, 299–317. https://doi.org/10.1007/BF02783144.

Price, C.J., Marr, M.C., Myers, C.B., Seely, J.C., Heindel, J.J., Schwetz, B.A., 1996a. The developmental toxicity of boric acid in rabbits. Fundam. Appl. Toxicol. 34, 176–187. https://doi.org/10.1006/faat.1996.0188.

Price, C.J., Strong, P.L., Marr, M.C., Myers, C.B., Murray, F.J., 1996b. Developmental toxicity NOAEL and postnatal recovery in rats fed boric acid during gestation. Fundam. Appl. Toxicol. 32, 179–193. https://doi.org/10.1006/faat.1996.0121.

Rajendran, K.G., Chen, S.Y., Sood, A., Spielvogel, B.F., Hall, I.H., 1995. The anti-osteoporotic activity of amine-carboxyboranes in rodents. Biomed. Pharmacother. 49, 131–140. https://doi.org/10.1016/0753-3322(96)82606-0.

Reiss, D., Beyer, K., Engelmann, B., 1997. Delayed oxidative degradation of polyunsaturated diacyl phospholipids in the presence of plasmalogen phospholipids in vitro. Biochem. J. 323, 807–814. https://doi.org/10.1042/bj3230807.

Robbins, W.A., Xun, L., Jia, J., Kennedy, N., Elashoff, D.A., Ping, L., 2010. Chronic boron exposure and human semen parameters. Reprod. Toxicol. 29, 184–190. https://doi.org/10.1016/j.reprotox.2009.11.003.

Rousseau, A.S., Sibille, B., Murdaca, J., Mothe-Satney, I., Grimaldi, P.A., Neels, J.G., 2016. α-Lipoic acid up-regulates expression of peroxisome proliferator-activated receptor β in skeletal muscle: involvement of the JNK signaling pathway. FASEB J. 30, 1287–1299. https://doi.org/10.1096/fj.15-280453.

Schiermeier, Q., 2008. Water: purification with a pinch of salt. Nature. 452, 260–261. https://doi.org/10.1038/452260a.

Scialli, A.R., Bonde, J.P., Brüske-Hohlfeld, I., Culver, B.D., Li, Y., Sullivan, F.M., 2010. An overview of male reproductive studies of boron with an emphasis on studies of highly exposed Chinese workers. Reprod. Toxicol. 29, 10–24. https://doi.org/10.1016/j.reprotox.2009.10.006.

Seal, B.S., Weeth, H.J., 1980. Effect of boron in drinking water on the male laboratory rat. Bull. Environ. Contam. Toxicol. 25, 782–789. https://doi.org/10.1007/BF01985608.

Sedlak, D.L., 2019. The unintended consequences of the reverse osmosis revolution. Environ. Sci. Technol. 53, 3999–4000. https://doi.org/10.1021/acs.est.9b01755.

Shearer, M.J., Newman, P., 2008. Metabolism and cell biology of vitamin K. Thromb. Haemost. 100, 530–547.

Simoni, M., Brigante, G., Rochira, V., Santi, D., Casarini, L., 2020. Prospects for FSH treatment of male infertility. J. Clin. Endocrinol. Metab. 1057 (7), dgaa243. https://doi.org/10.1210/clinem/dgaa243.

Tanaka, M., Fujiwara, T., 2008. Physiological roles and transport mechanisms of boron: perspectives from plants. Pflugers Arch. 456, 671–677. https://doi.org/10.1007/s00424-007-0370-8.

Treinen, K.A., Chapin, R.E., 1991. Development of testicular lesions in F344 rats after treatment with boric acid. Toxicol. Appl. Pharmacol. 1072 (2), 325–335. https://doi.org/10.1016/0041-008x(91)90212-w.

U.S. EPA, 2002. Iris Toxicological Review And Summary Documents For Boron And Compounds (Third External Review Draft 2002). https://cfpub.epa.gov/si/si_public_record_report.cfm?Lab=NCEA&dirEntryId=29528.

U.S. EPA, 2008a. Drinking Water Health Advisory For Boron. Document Number: EPA-822-R-08-013. https://www.epa.gov/sites/production/files/2014-09/documents/drinking_water_health_advisory_for_boron.pdf.

U.S. EPA, 2008b. Health Effects Support Document for Boron. Document Number: EPA-822-R-06-005. https://www.epa.gov/sites/production/files/2014-09/documents/health_effects_support_document_for_boron.pdf.

Vera, A., Moreno, J.L., García, C., Morais, D., Bastida, F., 2019. Boron in soil: the impacts on the biomass, composition and activity of the soil mi-crobial community. Sci. Total Environ. 685, 564–573. https://doi.org/10.1016/j.scitotenv.2019.05.375.

Wang, J., Zhu, H., Wang, K., Yang, Z., Liu, Z., 2020. Protective effect of quercetin on rat testes against cadmium toxicity by alleviating oxidative stress and autophagy. Environ. Sci. Pollut. Res. Int. 27, 25278–25286. https://doi.org/10.1007/s11356-020-08947-2.

Wang, X.J., Shen, C.L., Dyson, M.T., Yin, X.L., Schiffer, R.B., Grammas, P., Stocco, D.M., 2006. The involvement of epoxygenase metabolites of arachidonic acid in cAMP-stimulated steroidogenesis and steroidogenic acute regulatory protein gene expression. J. Endocrinol. 190, 871–878. https://doi.org/10.1677/joe.1.06933.

Weir Jr., R.J., Fisher, R.S., 1972. Toxicologic studies on borax and boric acid. Toxicol. Appl. Pharmacol. 23, 351–364. https://doi.org/10.1016/0041-008x(72)90037-3.

Wolska, J., Bryjak, M., 2013. Methods for boron removal from aqueous solutions — a review. Desalination. 310, 18–24. https://doi.org/10.1016/j.desal.2012.08.003.

Xiao, D., Zeng, L., Yao, K., Kong, X., Wu, G., Yin, Y., 2016. The glutamine-alpha-ketoglutarate (AKG) metabolism and its nutritional implications. Amino Acids 48, 2067–2080. https://doi.org/10.1007/s00726-016-2254-8.

Zárate, R., El Jaber-Vazdekis, N., Tejera, N., Pérez, J.A., Rodríguez, C., 2017. Significance of long chain polyunsaturated fatty acids in human health. Clin. Transl. Med. 6, 25. https://doi.org/10.1186/s40169-017-0153-6.

Zhang, H., Shao, X., Zhao, H., Li, X., Wei, J., Yang, C., Cai, Z., 2019. Integration of metabolomics and lipidomics reveals metabolic mechanisms of triclosan-induced toxicity in human hepatocytes. Environ. Sci. Technol. 53, 5406–5415. https://doi.org/10.1021/acs.est.8b07281.

Zhang, Y.L., wang, H.L., yu, X.W., Tong, Z.D., 2012. Surveillance data analysis of multi-sources of water and drinking water. J. Environ. Occup. Med. 29 (11), 681–688.

Zhao, L., Huang, Y., Adeleye, A.S., Keller, A.A., 2017. Metabolomics reveals cu(OH)2 nanopesticide activated antioxidative pathways and decreased beneficial antioxidants in spinach leaves. Environ. Sci. Technol. 51, 10184–10194. https://doi.org/10.1021/acs.est.7b02163.

SUPPORTING INFORMATION

Reproductive toxicity and metabolic perturbations in male rats exposed to boron

Chong Wang[a], Ziqing Kong[b], Lian Duan[a], Fuchang Deng[a], Yuanyuan Chen[a], Sheng Quan[b], Xiaohui Liu[c], Yu'e Cha[a], Yufeng Gong[d], Chao Wang[a,d], Ying Shi[a], Wen Gu[a], Yuanzheng Fu[a], Donghai Liang[e], John P. Giesy[d,f,g], Hongwei Zhang[a], Song Tang[a,h]*

[a] China CDC Key Laboratory of Environment and Population Health, National Institute of Environmental Health, Chinese Center for Disease Control and Prevention, Beijing 100021, China

[b] Calibra-Metabolon Joint Metabolomics Laboratory, Calibra Diagnostics Ltd., Hangzhou, Zhejiang 310000, China

[c] National Protein Science Technology Center and School of Life Sciences, Tsinghua University, Beijing 100084, China

[d] Toxicology Centre, University of Saskatchewan, Saskatoon, SK S7N 5B3, Canada

[e] Gangarosa Department of Environmental Health, Rollins School of Public Health, Emory University, Atlanta, GA 30322, USA

[f] Department of Biomedical and Veterinary Biosciences, University of Saskatchewan, Saskatoon, SK S7N 5B4, Canada

[g] Department of Environmental Science, Baylor University, Waco, TX 76798, USA

[h] Center for Global Health, School of Public Health, Nanjing Medical University, Nanjing, Jiangsu 211166, China

***Corresponding author:** No. 7 Panjiayuan Nanli, Chaoyang District, Beijing 100021, China. Tel: +86-10-5093-0101. E-mail: tangsong@nieh.chinacdc.cn (Dr. Song Tang).

Summary: 35 Pages, 7 Tables, and 3 Figures

Content

MATERIALS AND METHODS

Chemicals and Materials

Chloral hydrate (CAS 302-17-0) was from Oriental SaiRui Biotechnology Co., Ltd. (Beijing, China). ELISA kits for testicular 25-hydroxyvitamin D_3 (25[OH]D_3) and steroid hormones of testosterone (T), cortisol, estrone (E_1), estradiol (E_2), estriol (E_3), dehydroepiandrosterone (DHEA), androstendione (ASD), and aldosterone (ALD) were from Wuhan Colorful Gene biological technology company (Wuhan, Hubei, China). ELISA kits for plasma follicle-stimulating hormone (FSH), luteinizing hormone (LH) , testicular malate dehydrogenase (MDH), glyceraldehyde-3-phosphate dehydrogenase (G3PDH), sorbitol dehydrogenase (SDH)） and hyaluronidase (H) were all bought from Future Industrial Company (Shanghai, China). Bradford protein quantitative kit was from GENMED Scientifics Inc. (Shanghai, China). Rat Metabolic Hormone (RMHMAG084K) and Cytokine/Chemokine Magnetic Bead kits (RECYTMAG-65K) were provided by Merck Millipore (Billerica, MA, USA).

Animal Husbandry and Exposure

4 to 5 rats were maintained per cage (temperature 22-24°C; relative humidity 50-60%) with a 12/12 h light/dark cycle. Rats were fed a standard diet from Keaoxieli Feed Co., Ltd. (Beijing, China) and treated humanely for the alleviation of suffering. Since absorption of B through dermal and respiration is less than the average daily dietary intake, oral gavage was selected as the exposure route to assure the accurate delivery. Throughout the exposures,

daily-prepared fresh solutions were used, and body weight and food consumption were recorded at weekly intervals.

Quantification of Boron

Concentrations of B were determined in both plasma and water samples. 100 μL of them was added with 1.9 mL of 0.1% HNO_3 and 0.01% Triton. After mixture, samples were centrifuged at 3000×g for 5 mins. For dietary samples, 0.1 g sample was weighted and 1 mL of HNO_3 was added and left at room temperature for overnight. Deionized water was then added to reach 5 mL and digested for 1 hr in a water bath. After filtration, the supernatant of all samples was extracted. Testicular boron was digested with HNO_3 and H_2O_2 to obtain a colorless and transparent solution. B was quantified by use of Inductively Coupled Plasma Mass Spectrometer (iCAP RQ ICP-MS, Thermo Fisher, Waltham, MA, USA) and expressed as mg/kg wet weight in testes or μg/L in diet and plasma/water samples, respectively.

Male Fertility Assay

After 28 days exposure, the remaining male rats in each group (n=5) were caged individually with an untreated virgin proestrus female SD rat and housed together in a 1:1 ratio for a mating period of 7 days. During this period, female rats were confirmed with the presence of vaginal plugs every morning. Once insemination was confirmed, female rat was separated from the male and housed individually in a separate cage for 10 days gestation and replaced by another virgin proestrus female rat. At the end of 10 days, female rats were

sacrificed. Pregnancy rate, number of luteum, and abnormal rate of fetuses were examined and calculated. The gestation rate (%) = number of female rats that had fetal rats/number of pregnant female rats×100. The average fetus number = number of fetal rats/number of female rats that had fetal rats. The live fetus rate (%) = number of live fetus rats/number of fetal rats×100. The whole serial fertility and gestation process was repeated for 10 times and lasted for about 10 weeks, and totally 50 female rats were used in each group.

Histopathological Examination of Testis and Epididymis

Histopathology of testis and epididymis as well as the measurements of diameter of seminiferous tubule and cycle of spermatogenesis was conducted to assess reproductive effects by an experienced pathologist blinded to the sample identity. Left testis and paired epididymis (n=4) were removed and washed with cleaning solution, and then fixed in 4% paraformaldehyde. After washing, tissues were dehydrated and embedded in paraffin for sectioning. After cut into 4 μm slices, slides were stained with hematoxylin and eosin. Photomicrographs were taken with CX31 microscope (Olympus, Shanghai, China). Diameters of 100 seminiferous tubular with mature sperm were measured in each rat with Image View v3.7.7817 (Shunyu Instrument Co., Ltd., Ningbo, Zhejiang, China). Numbers of spermatogonia and primary spermatocytes in 10 proximal seminiferous tubules were counted in each rat.

Testicular Enzymes and Steroid Hormones Analysis

The dissected right testis was used to determine testicular enzymes and steroid hormones. It was washed with pre-chilled PBS (0.01 M, pH = 7.4) and weighed. Tissue was grinded with PBS with protein inhibitors. The homogenate was centrifuged at 5000×g for 10 mins and the supernatant was collected. Total protein concentration per sample was calculated according to the protocol of Bradford Protein Concentration Quantitation Kit. Testicular SDH, MDH, G3PDH, H, 25[OH]D_3, E_1, E_2, E_3, T, cortisol, DHEA, ASD, and ALD (n=4) were determined following ELISA kit protocol. OD values were measured at a wavelength of 450 nm using a Varioskan Flash Spectral Scanning Multimode Reader (Thermo Scientific, MA, USA). Based on the calibration curves of standards, testicular enzyme activities were determined in each sample.

Plasma Hormone and Cytokine Analyses

Plasma Gonadotropin of FSH and LH (n=8) were determined following ELISA kit protocol, which was the same as afore testicular enzyme assay. Milliplex MAP Rat Cytokine/Chemokine Magnetic Bead 15-plex Panel [interleukins (IL-1α，IL-1β，IL-2，IL-4，IL-5，IL-12，and IL-17)，interferon (IFN-γ), colony stimulating factor (G-CSF and GM-CSF), growth factor (EGF and VEGF-A), and chemokines (IP-10, RANTES/CCL5 and Eotaxin/CCL11] and Metabolic Hormone Magnetic Bead 9-plex Panel [interleukin IL-6, tumor necrosis factor TNF-γ, chemokine MCP-1, metabolic hormones (Leptin, Insulin, Pancreatic Polypeptice (PP), PYY, GIP, and C-Peptide)] were used for analysis of 25 μL

plasma (n=5) according to the manufacturer's instruction. All measurements were performed on a MAGPIX Luminex instrument using xPonent 4.2 (Luminex) and Bio-Plex Manager 6.1 softwares (Bio-Rad, Hercules, CA, USA). Unless specified otherwise, plasmas were diluted 1:2 in assay buffer for cytokine kit and no dilution for metabolic hormone kit. Plate was wrapped with foil and incubated for 2 hrs at room temperature for cytokine kit, while incubated with agitation on a plate shaker overnight (18-20 hrs) at 4°C for metabolic hormone kit. Median Fluorescent Intensity (MFI) data was analyzed using a 5-parameter logistic or spline curve-fitting method for calculating analyte concentrations in each sample.

Non-target Metabolomics and Data Processing

Non-targeted metabolomics of plasma samples (n=5) was performed at Calibra-Metabolon Joint Metabolomics Laboratory (Hangzhou, Zhejiang, China) by using 100 μL plasma. Sample handling, quality control (QC), metabolite identification, data curation, quantification and data normalizations were following previous studies.[1] Recovery standards were added prior to the extraction process for QC. For the metabolite extraction, proteins were precipitated with methanol under vigorous shaking for 2 mins (GenoGrinder 2000, Swedesboro, NJ, USA) followed by centrifugation. The resulting extract was divided into five fractions: two for analysis by two separate reverse phase (RP)/UPLC-MS/MS methods with positive ion mode electrospray ionization (ESI), one for analysis by RP/UPLC-MS/MS with negative ion mode ESI, one for analysis by HILIC/UPLC-MS/MS with negative ion mode ESI, and one was reserved for backup. Samples were placed briefly

on a TurboVap® (Zymark) to remove organic solvent. Sample extracts were stored overnight under nitrogen before analysis.

All methods utilized a Waters ACQUITY ultra-performance liquid chromatography (UPLC) and a Q-Exactive high resolution/accurate mass spectrometer (Thermo Fisher, Waltham, MA, USA) interfaced with a heated electrospray ionization (HESI-II) source and Orbitrap mass analyzer operated at 35,000 mass resolution. Sample extract was dried then reconstituted in solvents compatible to each of the four methods. Each reconstitution solvent contained a series of standards at fixed concentrations to ensure injection and chromatographic consistency. First aliquot was analyzed using acidic positive ion conditions, chromatographically optimized for more hydrophilic compounds. In this method, the extract was gradient eluted from a C18 column (Waters UPLC BEH C18-2.1x100 mm, 1.7 µm) using water and methanol, containing 0.05% perfluoropentanoic acid (PFPA) and 0.1% formic acid (FA). Second aliquot was also analyzed using acidic positive ion conditions; however, it was chromatographically optimized for more hydrophobic compounds. In this method, the extract was gradient eluted from C18 column using methanol, acetonitrile, water, 0.05% PFPA and 0.01% FA and was operated at an overall higher organic content. Third aliquot was analyzed using basic negative ion optimized conditions using a separate dedicated C18 column. The basic extracts were gradient eluted from the column using methanol and water, however with 6.5 mM Ammonium Bicarbonate at pH 8. Fourth aliquot was analyzed via negative ionization following elution from a HILIC column (Waters UPLC BEH Amide 2.1x150 mm, 1.7 µm) using a gradient consisting of water and acetonitrile with 10 mM Ammonium Formate, pH 10.8. The MS analysis alternated between MS and

data-dependent MSn scans using dynamic exclusion. The scan range varied slighted between methods but covered 70-1000 m/z.

Raw data was extracted, peak-identified and QC processed using Metabolon's (Research Triangle Park, NC, USA) hardware and software. Compounds were identified by comparison to library entries of purified standards or recurrent unknown entities. Metabolon maintains a library based on authenticated standards that contains the retention time/index (RI), mass to charge ratio (*m/z)*, and chromatographic data (including MS/MS spectral data) on all molecules present in the library. Furthermore, biochemical identifications were based on three criteria: (1) retention index within a narrow RI window of the proposed identification, (2) accurate mass match to the library+/-10ppm, and (3) the MS/MS forward and reverse scores between the experimental data and authentic standards. The MS/MS scores were based on a comparison of the ions present in the experimental spectrum to the ions present in the library spectrum. Peaks were quantified using area-under-the-curve.

Lipidomics and Data Processing

Lipidomics of plasma samples (n=5) were performed for each group, and lipid extraction was performed as described previously.[2] For each sample, 100 µL plasma was added to 400 µL $CHCl_3$:MeOH (2:1) and vortexed three times. After centrifugation at 3000×rpm for 15 mins at 4°C, the same volume of organic solvents was added. The lower phase was transferred to a new glass tube and water phase was added according to the proportion of water phase/organic phase (1:4). After extraction, excess protein was washed off and vortexed for three times. Extracted samples were centrifugated at 3000 rpm for 15 min at

4°C. The lower phase was extracted and dried at 4°C using nitrogen blowing and stored at -80°C for latter analysis. Lipid analyses were performed on a Q-Exactive orbitrap mass spectrometer with XSelect CSH C18 column at 45°C. Mobile phase A was prepared by dissolving 0.77 g of ammonium acetate in 400 mL of HPLC-grade water, followed by adding 600 mL of HPLC-grade acetonitrile. Mobile phase B was prepared by mixing 100 mL of acetonitrile with 900 mL isopropanol. Gradient was generated with flow rate at 250 μL/min. Lipids were identified and quantified using LipidSearch 4.1.30 (Thermo Fisher, Waltham, MA, USA). Mass tolerances of 5 ppm and 10 ppm were applied for precursor and product ions, respectively. Retention time shift of 0.25 min was performed in "alignment". M-score and chromatographic areas were used to reduce false positives. False positives were checked manually and eliminated based on the M-score and chromatographic behavior.[3] After data filtering, normalization to lipid internal standards representative of the analyte class was performed. Half of the minimum values among all the samples were used to replace the missing values.

QA/QC of Non-target Metabolomics and Lipidomics

Three types of controls were analyzed in concert with the experimental samples: (1) extracted water samples served as process blanks; (2) a pooled matrix sample generated by taking 10 μL of each plasma sample served as a technical replicate throughout the dataset;; and (3) a cocktail of QC standards that were carefully chosen not to interfere with the measurement of endogenous compounds were spiked into every analyzed sample, allowed instrument performance monitoring and aided chromatographic alignment. Instrument

variability was determined by calculating the median relative standard deviation (RSD) for the standards that were added to each sample prior to injection into the mass spectrometers. Overall process variability was determined by calculating the median RSD for all endogenous metabolites (i.e., non-instrument standards) present in 100% of the pooled matrix samples. All the experimental samples were randomized across the platform run with QC samples spaced evenly among the injections.

Table S1. Weekly changes in body mass (BM) of adult male rats exposed by gavage to boron at 0, 25, 50 and 100 mg/kg/day for 28 days. All values are expressed as mean ± S.D. (n=17) per group. Compared with the control, significance was determined at *p* values <0.05* and <0.01** by Student's t-test.

Group	**Initial BM (g)**	**1 Week BM (g)**	**2 Week BM (g)**	**3 Week BM (g)**	**Final BM (g)**	**BM Growth Rate (%)**
0	219.00±6.37	297.44±6.12	350.38±10.71	374.94±30.23	397.81±18.83	44.87±2.21
25	217.83±7.39	291.56±10.15	343.39±11.56	380.39±10.10	387.67±17.37	43.72±2.76
50	218.22±8.64	297.56±7.69	350.72±11.42	381.00±29.25	386.44±14.59	43.46±2.90
100	215.00±6.31	**288.00±11.78****	**341.89±12.94***	375.94±15.24	395.00±16.04	45.47±3.06

Table S2. Changes in organ masses of male rats exposed by gavage to boron at 0, 25, 50 and 100 mg/kg/day for 28 days. All values are expressed as mean ± S.D. (n=4) per group. Wet masses of epididymis, testis, liver, kidney, heart, lung, and spleen were recorded to calculate viscera coefficient by using the following formula: Viscera coefficient = (Organ mass/Total body weight) ×100%. Compared with the control, significance was determined at $p<0.05$* by Student's t-test.

Group	**Epididymis (g)**	**Testis (g)**	**Liver (g)**	**Kidney (g)**	**Heart (g)**	**Lung (g)**	**Spleen (g)**	**Epididymis (%BW)**	**Testis (%BW)**	**Liver (%BW)**	**Kidney (%BW)**	**Heart (%BW)**	**Lung (%BW)**	**Spleen (%BW)**
0	0.90±0.08	3.08±0.24	11.00±0.80	2.68±0.17	1.45±0.10	1.50±0.08	0.78±0.17	0.23±0.02	0.79±0.06	2.83±0.13	0.69±0.04	0.37±0.02	0.39±0.02	0.20±0.04
25	0.85±0.13	3.05±0.13	10.55±0.45	2.60±0.23	1.43±0.13	1.48±0.10	0.93±0.05	0.23±0.04	0.81±0.06	2.79±0.10	0.69±0.04	0.38±0.03	0.39±0.02	0.24±0.02
50	0.88±0.10	3.08±0.17	11.80±0.64	2.88±0.32	1.38±0.21	1.55±0.13	0.93±0.05	0.23±0.02	0.80±0.03	3.09±0.51	0.75±0.11	0.36±0.06	0.40±0.04	0.24±0.02
100	0.88±0.10	2.90±0.22	10.83±0.62	2.70±0.16	1.30±0.08	1.63±0.13	0.90±0.14	0.22±0.02	0.72±0.05	2.71±0.29	0.68±0.07	**0.33±0.03***	0.41±0.03	0.23±0.04

Table S3. No significant changes in seminiferous tubular diameter and number of spermatogenesis-related cells of male rats exposed by gavage to boron at 0, 25, 50 and 100 mg/kg/day for 28 days. The diameters of 100 seminiferous tubules were measured in each male rat. Numbers of spermatogonia and primary spermatocytes in 10 proximal seminiferous tubules of each rat were counted. All values are expressed as mean ± S.D. (n=4) in each group.

Group	**Seminiferous tubular diameter (μm)**	**Number of spermatogonia**	**Number of primary spermatocytes**
0	261.9±12.2	42±3	206±12
25	270.2±6.4	43±3	253±44
50	266.5±6.5	40±2	231±19
100	267.8±15.4	41±2	239±20

Table S4. Concentrations of boron in plasma and testis of male rats exposed by gavage to boron at 0, 25, 50 and 100 mg/kg/day for 28 days as well as in water and diet samples (n=4 or 5) that were measured by ICP-MS.

Samples	Concentrations	Sample Types
0-1	34.7 μg/L	Plasma
0-2	29.2 μg/L	Plasma
0-3	30.2 μg/L	Plasma
0-4	26.1 μg/L	Plasma
25-1	117 μg/L	Plasma
25-2	154 μg/L	Plasma
25-3	119 μg/L	Plasma
25-4	107 μg/L	Plasma
25-5	168 μg/L	Plasma
50-1	185 μg/L	Plasma
50-2	289 μg/L	Plasma
50-3	262 μg/L	Plasma
50-4	257 μg/L	Plasma
50-5	220 μg/L	Plasma
100-1	367 μg/L	Plasma
100-2	409 μg/L	Plasma
100-3	375 μg/L	Plasma
100-4	439 μg/L	Plasma
100-5	522 μg/L	Plasma
Water-1	37.1 μg/L	Water
Water-2	35.8 μg/L	Water
Water-3	37.2 μg/L	Water
Water-4	41.7 μg/L	Water
Diet-1	5.29 mg/kg	Diet
Diet-2	5.30 mg/kg	Diet
Diet-3	5.42 mg/kg	Diet
Diet-4	5.38 mg/kg	Diet
0-1	50.4 mg/kg	Testis
0-2	37.3 mg/kg	Testis
0-3	38.1 mg/kg	Testis
0-4	11.3 mg/kg	Testis
25-1	35.2 mg/kg	Testis
25-2	17.7 mg/kg	Testis
25-3	86.8 mg/kg	Testis
25-4	36.9 mg/kg	Testis
50-1	48.6 mg/kg	Testis
50-2	22.1 mg/kg	Testis
50-3	57.6 mg/kg	Testis
50-4	24.5 mg/kg	Testis
100-1	61.2 mg/kg	Testis
100-2	31.9 mg/kg	Testis
100-3	22.6 mg/kg	Testis
100-4	25.7 mg/kg	Testis

Figure S1. No significant changes in histopathology of testis, epididymis, seminiferous tubules and spermatogenic cells in male rats exposed by gavage to boron at 0, 25, 50 and 100 mg/kg/day for 28 days (n=4). (A) The spermatozoa of testes developed well, and mature sperm was formed in each group. The supporting cells and interstitial cells showed no proliferation, and no abnormal changes (H&E, × 100). (B) After exposure, there were no abnormalities in the structure of epididymis and output tubules of male rats in each experimental group. A large number of mature spermatozoa were observed in the lumen. The spermatozoa of male testes in all three-exposure groups developed well and mature sperm was found (H&E, × 100). (C) The spermatogenic tubules were intact and the diameter of the seminiferous tubules was normal (H&E, × 100). (D) The spermatogenic tubules with well-defined cells and mature sperm were chosen to count spermatogonia and primary spermatocytes. The small cuboidal or elliptical spermatogonia was located on the basement membrane and the nucleus of the primary spermatocyte was large or round that slightly colored in which interlaced globular chromosomes lied. No significant changes related to borax exposure (H&E, × 400). 1, 2, 3 and 4 in each panel represents groups of control, 25, 50, and 100 mg/kg, respectively. (E) The sperm, spermatogonia, and primary spermatocyte in D-1 were shown as arrows.

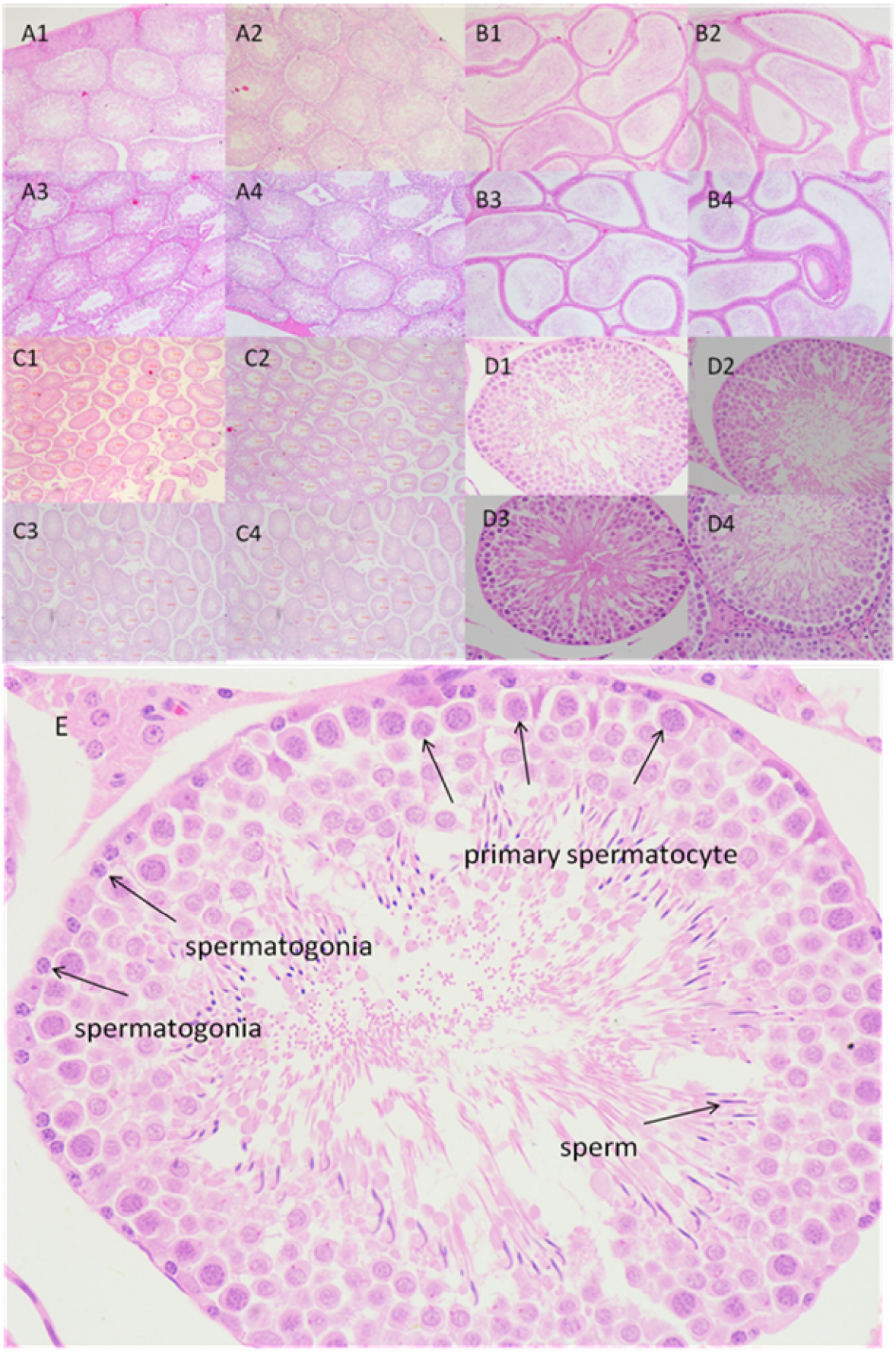
A1
A2
B1
B2
A3
A4
B3
B4
C1
C2
D1
D2
C3
C4
D3
D4
E
primary spermatocyte
spermatogonia
spermatogonia
sperm

Figure S2. No significant changes in levels of plasma cytokine (IL-1α, IL-1β, IL-2, IL-4, IL-6, IL-12, IL-17, IP-10, IFN-γ, TNF-α, G-CSF, GM-CSF, MCP-1, Eotaxin and RANTES) or metabolic hormone (Leptin, Insulin, Pancreatic Polypeptice, PYY, GIP and C-Peptide) and LH (gonadotropins) as well as testicular enzyme HA that is related to spermatogenesis in male rats exposed by gavage to boron at 0, 25, 50 and 100 mg/kg/day for 28 days (n=5). Significance was determined at *p* values <0.05 by one-way ANOVA followed by t-test.

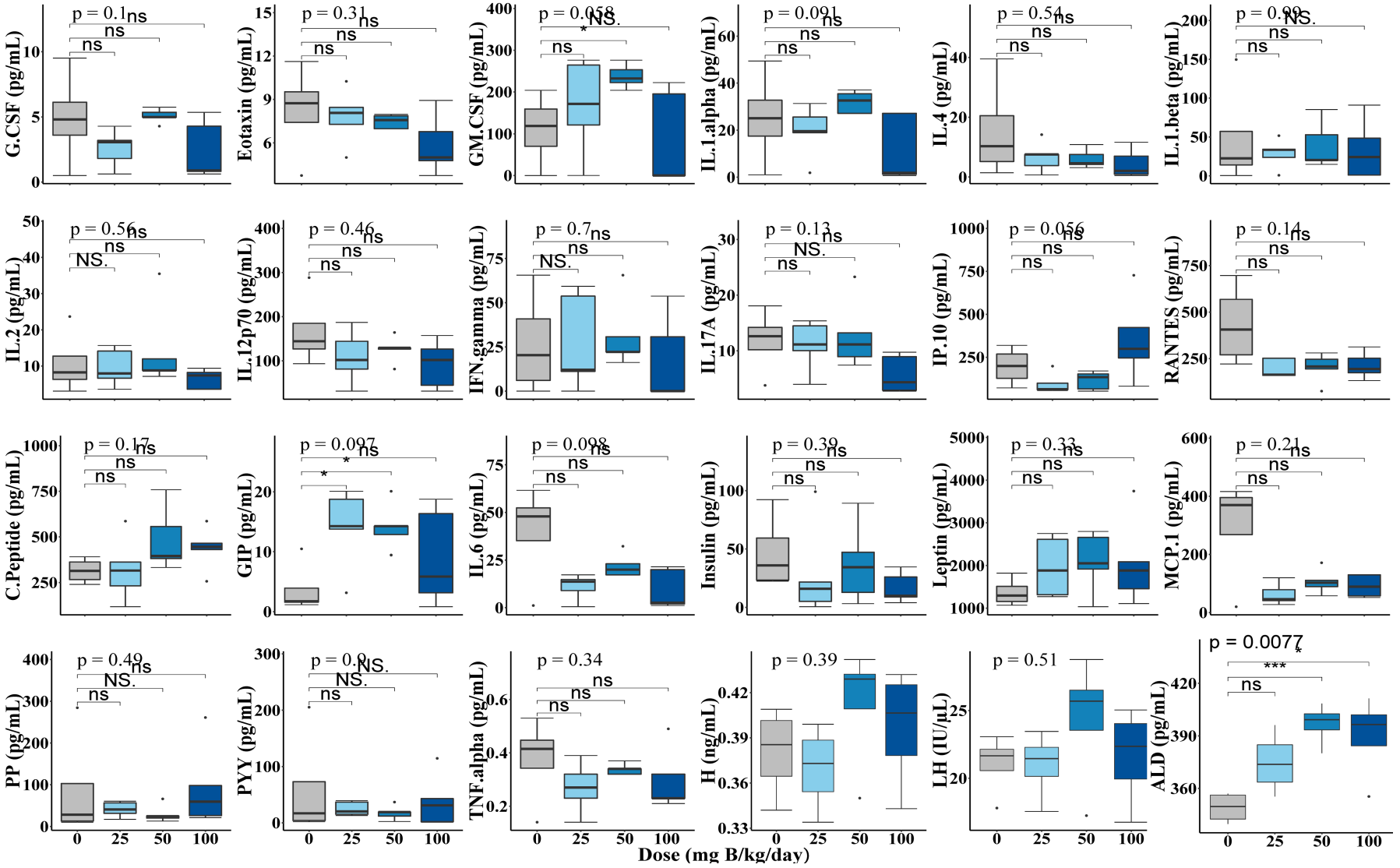

Figure S3. Heatmap of the significantly changed plasma metabolites and lipids in male rats exposed by gavage to boron at 0, 25, 50 and 100 mg/kg/day for 28 days using untargeted metabolomics (top) and lipidomics (bottom).

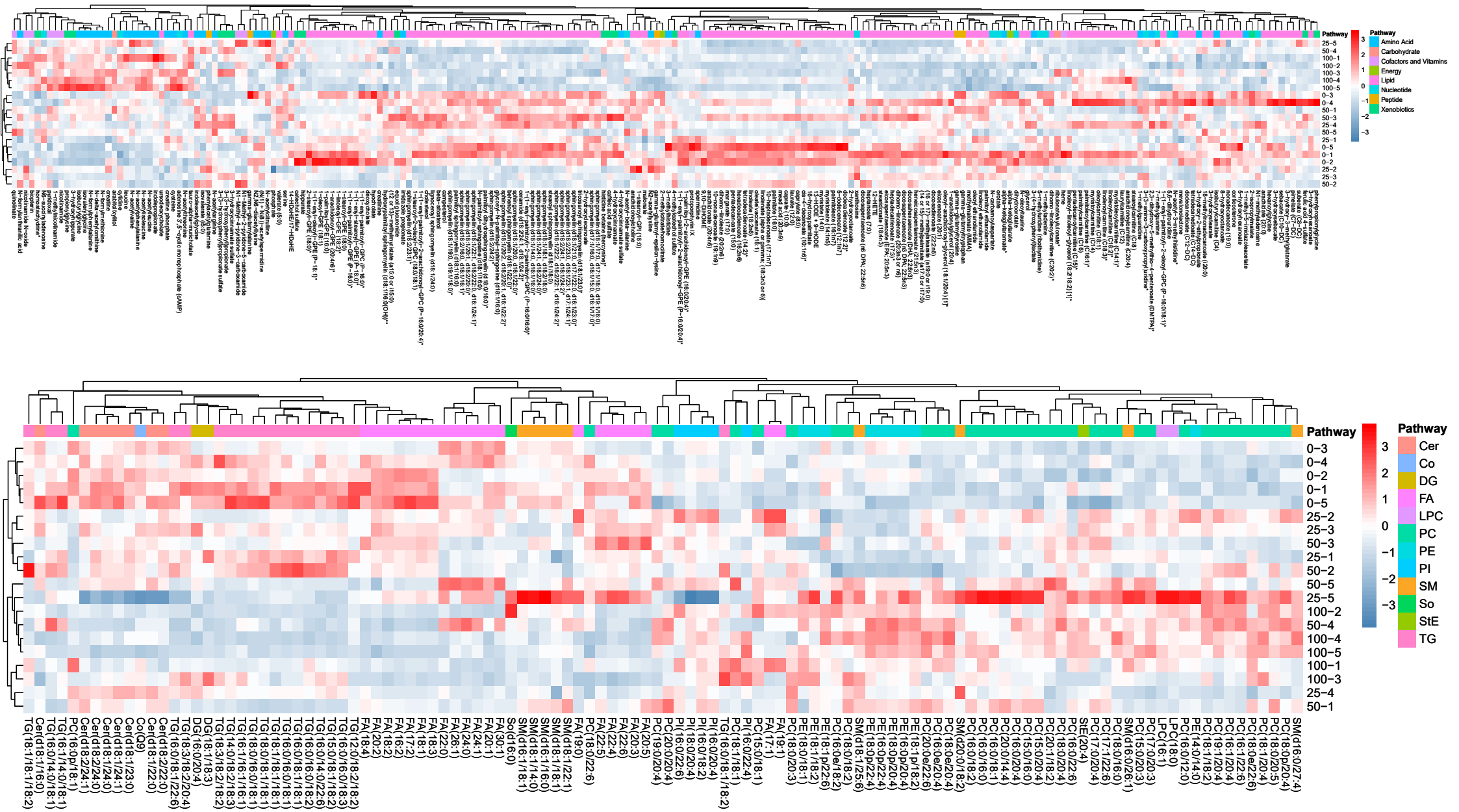

Table S5. Numbers of significantly (FDR_{B-H}<0.05) changed plasma metabolites in male rats exposed by gavage to boron at 0, 25, 50 and 100 mg/kg/day for 28 days using untargeted metabolomics and lipidomics.

Statistically Significant Metabolites	**Statistical Comparisons**		
	25 vs 0	**50 vs 0**	**100 vs 0**
Plasma Metabolomics FDR<0.05	64	76	192
Metabolites (↑|↓)	8|56	17|59	31|161
Plasma Lipidomics FDR<0.05	16	27	95
Metabolites (↑|↓)	10|6	19|8	44|51

Table S6. List of significantly changed plasma metabolites in male rats exposed by gavage to boron at 0, 25, 50 and 100 mg/kg/day for 28 days using untargeted metabolomics.

Pathway	Sub-pathway	Compound	HMDB	RI	M/Z	Mode	Fold of Change			*P* Value			*FDR*		
							25	50	100	25	50	100	25	50	100
Amino Acid	Glycine, Serine and Threonine	serine	HMDB00187	1239	106.050	pos	0.87	0.96	0.93	0.012	0.323	0.216	0.357	0.555	0.178
	Metabolism	N-acetylthreonine	HMDB62557	821.6	160.062	neg	1.01	0.99	1.23	0.838	0.937	0.027	0.631	0.800	0.055
	Glutamate Metabolism	alpha-ketoglutaramate*	HMDB0001552	1916	144.030	neg	0.86	0.75	0.70	0.243	0.028	0.031	0.461	0.323	0.059
	Histidine Metabolism	3-methylhistidine	HMDB00479	906.3	168.078	neg	0.87	0.81	0.63	0.553	0.332	0.043	0.575	0.562	0.070
		N-acetyl-3-methylhistidine*		2056	212.103	pos	0.60	0.67	0.77	0.037	0.107	0.267	0.361	0.407	0.203
		imidazole propionate	HMDB02271	2263	141.066	pos	1.07	1.26	0.29	0.696	0.525	0.003	0.608	0.650	0.018
		1-methyl-5-imidazoleacetate	HMDB04988	1989	141.066	pos	0.94	0.80	0.58	0.611	0.083	0.017	0.595	0.391	0.041
	Lysine Metabolism	N2-acetyllysine	HMDB00446	3372.6	187.109	neg	0.95	0.84	0.64	0.661	0.165	0.010	0.608	0.453	0.030
		N2, N6-diacetyllysine		1604	229.119	neg	0.80	0.72	0.63	0.179	0.021	0.004	0.438	0.288	0.018
	Phenylalanine Metabolism	N-acetylphenylalanine	HMDB00512	2597	206.082	neg	1.15	0.99	1.81	0.799	0.903	0.017	0.624	0.789	0.042
	Tyrosine Metabolism	3-(4-hydroxyphenyl)lactate	HMDB00755	1379	181.051	neg	0.94	0.88	0.80	0.397	0.071	0.038	0.530	0.391	0.065
		N-formylphenylalanine	HMDB0240317	2360	192.067	neg	1.69	2.29	3.27	0.116	0.039	0.015	0.380	0.364	0.039
		4-hydroxycinnamate sulfate		1000	242.997	neg	0.47	0.75	0.13	0.060	0.306	0.000	0.361	0.545	0.006
	Tryptophan Metabolism	N-formylanthranilic acid	HMDB04089	2150	164.035	neg	1.20	1.60	1.36	0.255	0.000	0.032	0.461	0.151	0.059
		indolepropionate	HMDB02302	3205	190.086	pos	0.91	1.00	1.75	0.487	0.996	0.020	0.556	0.804	0.046
		indoleacetylglycine		2610	231.078	neg	1.15	1.33	1.03	0.299	0.019	0.758	0.482	0.279	0.377
	Leucine, Isoleucine and Valine	leucine	HMDB00687	2864	132.102	pos	1.07	1.13	1.22	0.115	0.031	0.003	0.380	0.323	0.018
	Metabolism	N-acetylleucine	HMDB11756	2400	172.098	neg	1.40	1.31	2.43	0.164	0.167	0.002	0.422	0.453	0.014
		isovalerate (i5:0)	HMDB00718	1564	101.061	neg	1.24	1.35	1.04	0.090	0.012	0.690	0.374	0.279	0.358
		isovalerylglycine	HMDB00678	1950	158.082	neg	1.54	2.08	3.17	0.148	0.050	0.015	0.406	0.374	0.040
		N-acetylisoleucine	HMDB61684	2325	172.098	neg	1.38	1.27	2.21	0.089	0.167	0.001	0.374	0.453	0.011
		3-hydroxy-2-ethylpropionate	HMDB00396	975	117.056	neg	0.89	0.82	0.54	0.325	0.021	0.025	0.503	0.288	0.050
		N-acetylvaline	HMDB11757	1704	158.082	neg	1.22	1.02	1.33	0.245	0.961	0.047	0.461	0.804	0.073
		isobutyrylcarnitine (C4)	HMDB00736	2810	232.154	pos	0.93	0.72	0.68	0.552	0.018	0.006	0.575	0.279	0.022
		isobutyrylglycine	HMDB00730	1420	144.067	neg	1.51	1.98	3.19	0.152	0.053	0.013	0.413	0.374	0.035

	Methionine, Cysteine, SAM and Taurine	N-formylmethionine	HMDB01015	1543.8	176.039	neg	1.47	1.94	2.82	0.164	0.048	0.014	0.422	0.374	0.037
	Metabolism	2,3-dihydroxy-5-methylthio-4-pentenoate (DMTPA)*	HMDB0240388	1156	177.023	neg	1.00	0.97	0.83	0.968	0.670	0.047	0.666	0.723	0.073
		cysteine	HMDB00574	1475	122.027	pos	1.34	1.07	1.80	0.016	0.426	0.002	0.357	0.605	0.013
	Urea cycle; Arginine and Proline	N-acetylarginine	HMDB04620	2245	217.130	pos	1.34	1.68	1.06	0.227	0.027	0.805	0.451	0.322	0.387
	Metabolism	N-acetylcitrulline	HMDB00856	940	216.099	neg	0.96	0.78	0.89	0.697	0.046	0.303	0.608	0.369	0.219
		N-delta-acetylornithine		858	173.093	neg	1.47	1.86	2.50	0.140	0.023	0.005	0.406	0.304	0.020
	Creatine Metabolism	creatine	HMDB00064	1947	132.077	pos	0.97	0.96	1.12	0.682	0.537	0.039	0.608	0.656	0.065
		creatinine	HMDB00562	2055	114.066	pos	0.90	0.93	0.87	0.005	0.134	0.006	0.357	0.435	0.022
		creatine phosphate	HMDB01511	660	212.043	pos	1.24	1.03	1.72	0.698	0.850	0.021	0.608	0.780	0.046
	Polyamine Metabolism	spermidine	HMDB01257	3355	146.165	pos	0.76	0.39	0.41	0.447	0.018	0.021	0.555	0.279	0.046
		(N(1) + N(8))-acetylspermidine		3080	188.176	pos	1.00	0.67	0.65	0.883	0.017	0.016	0.641	0.279	0.040
	Guanidino and Acetamido Metabolism	1-methylguanidine	HMDB01522	2149	74.071	pos	0.91	0.85	0.62	0.599	0.450	0.048	0.592	0.614	0.074
Peptide	Gamma-glutamyl Amino Acid	gamma-glutamylalanine	HMDB29142	1986	219.098	pos	0.77	0.61	0.37	0.744	0.308	0.041	0.614	0.546	0.068
		gamma-glutamyl-epsilon-lysine	HMDB03869	2725	276.155	pos	1.08	1.00	0.73	0.661	0.948	0.044	0.608	0.804	0.071
		gamma-glutamyltryptophan	HMDB29160	1960	332.125	neg	0.82	0.86	0.58	0.042	0.153	0.000	0.361	0.448	0.006
		gamma-glutamyltyrosine	HMDB11741	2518	311.124	pos	0.85	0.87	0.69	0.144	0.240	0.006	0.406	0.502	0.022
	Acetylated Peptides	phenylacetylglutamine	HMDB06344	2330	263.104	neg	1.34	1.12	0.60	0.112	0.741	0.024	0.380	0.740	0.050
Carbohydrate	Pentose Metabolism	arabitol/xylitol	HMDB0001851	1932.4	151.061	neg	1.01	1.24	1.40	0.946	0.231	0.042	0.662	0.499	0.069
		ribulonate/xylulonate*	HMDB0000867	2350	165.040	neg	0.78	0.56	0.77	0.249	0.004	0.192	0.461	0.230	0.164
Energy	TCA Cycle	alpha-ketoglutarate	HMDB00208	2700	145.014	neg	0.81	0.71	0.53	0.382	0.150	0.021	0.526	0.448	0.046
		2-methylcitrate/homocitrate	HMDB0000379	575	205.035	neg	0.85	0.73	0.37	0.519	0.358	0.036	0.567	0.584	0.063
	Oxidative Phosphorylation	phosphate	HMDB01429	608	96.970	neg	0.89	1.17	1.02	0.462	0.045	0.825	0.555	0.369	0.393
Lipid	Fatty Acid Synthesis	malonate	HMDB00691	3447	103.004	neg	0.92	1.05	0.76	0.515	0.586	0.035	0.567	0.680	0.063
	Short Chain Fatty Acid	valerate (5:0)	HMDB00892	1718	101.061	neg	1.07	1.53	1.01	0.959	0.033	0.544	0.665	0.330	0.311
		heptanoate (7:0)	HMDB00666	3670	129.092	neg	0.73	0.86	0.62	0.077	0.429	0.018	0.374	0.606	0.042
		caprylate (8:0)	HMDB00482	4362	143.108	neg	0.90	0.86	0.70	0.494	0.362	0.030	0.559	0.584	0.058
	Medium Chain Fatty Acid	caprate (10:0)	HMDB00511	5090.7	171.139	neg	0.74	0.85	0.53	0.094	0.389	0.005	0.374	0.586	0.020
		cis-4-decenoate (10:1n6)*	HMDB0004980	4890	169.123	neg	0.65	0.58	0.55	0.083	0.068	0.030	0.374	0.391	0.058
		laurate (12:0)	HMDB00638	5300	199.170	neg	0.78	0.85	0.63	0.080	0.253	0.004	0.374	0.507	0.018

	5-dodecenoate (12:1n7)	HMDB00529	5224	197.155	neg	0.51	0.54	0.33	0.112	0.141	0.021	0.380	0.440	0.046
Long Chain Fatty Acid	myristate (14:0)	HMDB00806	5440	227.202	neg	0.68	0.73	0.58	0.084	0.174	0.025	0.374	0.453	0.050
	myristoleate (14:1n5)	HMDB02000	5346.9	225.186	neg	0.51	0.54	0.34	0.058	0.081	0.008	0.361	0.391	0.027
	pentadecanoate (15:0)	HMDB00826	5521	241.217	neg	0.81	0.79	0.72	0.093	0.045	0.009	0.374	0.369	0.029
	palmitate (16:0)	HMDB00220	5618	255.233	neg	0.65	0.76	0.57	0.065	0.226	0.020	0.369	0.499	0.046
	palmitoleate (16:1n7)	HMDB03229	5475	253.217	neg	0.48	0.54	0.31	0.085	0.139	0.016	0.374	0.439	0.040
	margarate (17:0)	HMDB02259	5731	269.249	neg	0.73	0.77	0.66	0.047	0.082	0.007	0.361	0.391	0.023
	10-heptadecenoate (17:1n7)	HMDB60038	5555	267.233	neg	0.54	0.60	0.37	0.041	0.083	0.003	0.361	0.391	0.017
	oleate/vaccenate (18:1)	HMDB0003231	5655	281.249	neg	0.52	0.61	0.39	0.024	0.081	0.003	0.357	0.391	0.017
	nonadecanoate (19:0)	HMDB00772	6068	297.280	neg	0.78	0.82	0.69	0.078	0.029	0.000	0.374	0.323	0.005
	10-nonadecenoate (19:1n9)	HMDB13622	5780	295.264	neg	0.60	0.67	0.41	0.032	0.060	0.000	0.357	0.378	0.005
	arachidate (20:0)	HMDB02212	6240	311.296	neg	0.92	0.90	0.79	0.180	0.019	0.021	0.438	0.279	0.046
	eicosenoate (20:1)	HMDB02231	5950	309.280	neg	0.63	0.68	0.39	0.025	0.005	0.000	0.357	0.230	0.004
	heptadecatrienoate (17:3)*		5390	263.202	neg	0.52	0.67	0.31	0.100	0.252	0.005	0.374	0.507	0.020
Polyunsaturated Fatty Acid (n3 and n6)	heneicosapentaenoate (21:5n3)		5514	315.233	neg	0.56	0.86	0.44	0.050	0.515	0.010	0.361	0.647	0.029
	tetradecadienoate (14:2)*	HMDB00560	5292	223.170	neg	0.59	0.63	0.43	0.060	0.095	0.006	0.361	0.391	0.022
	hexadecadienoate (16:2n6)	HMDB00477	5398	251.202	neg	0.55	0.59	0.42	0.063	0.083	0.006	0.363	0.391	0.022
	stearidonate (18:4n3)	HMDB06547	5395	275.202	neg	0.48	0.58	0.31	0.025	0.091	0.001	0.357	0.391	0.011
	eicosapentaenoate (EPA; 20:5n3)	HMDB01999	5450	301.217	neg	0.69	0.86	0.53	0.096	0.472	0.010	0.374	0.631	0.031
	docosapentaenoate (n3 DPA; 22:5n3)	HMDB06528	5571	329.249	neg	0.74	0.86	0.43	0.219	0.497	0.004	0.451	0.647	0.018
	docosahexaenoate (DHA; 22:6n3)	HMDB02183	5525	327.233	neg	0.64	0.91	0.53	0.041	0.581	0.005	0.361	0.679	0.019
	linoleate (18:2n6)	HMDB00673	5535	279.233	neg	0.55	0.62	0.42	0.040	0.054	0.002	0.361	0.374	0.013
	linolenate [alpha or gamma; (18:3n3 or 6)]	HMDB03073	5450	277.217	neg	0.51	0.57	0.35	0.043	0.071	0.002	0.361	0.391	0.014
	dihomo-linolenate (20:3n3 or n6)	HMDB02925	5596	305.249	neg	0.65	0.75	0.44	0.059	0.197	0.002	0.361	0.487	0.013
	arachidonate (20:4n6)	HMDB01043	5535	303.233	neg	0.74	0.81	0.64	0.069	0.163	0.005	0.369	0.453	0.020
	docosapentaenoate (n6 DPA; 22:5n6)	HMDB01976	5624.5	329.249	neg	0.49	0.84	0.50	0.004	0.372	0.012	0.357	0.585	0.034
	docosadienoate (22:2n6)	HMDB61714	6034	335.296	neg	0.78	0.74	0.56	0.057	0.006	0.000	0.361	0.230	0.005
	dihomo-linoleate (20:2n6)	HMDB05060	5730	307.264	neg	0.63	0.69	0.45	0.033	0.073	0.001	0.357	0.391	0.011
	mead acid (20:3n9)	HMDB10378	5650	305.249	neg	0.40	0.62	0.39	0.015	0.166	0.010	0.357	0.453	0.031

Fatty Acid, Branched	18-methylnonadecanoate (i20:0)		6170	311.296	neg	0.77	0.83	0.30	0.300	0.406	0.001	0.482	0.590	0.011
	(12 or 13)-methylmyristate (a15:0 or i15:0)		5499	241.217	neg	0.98	1.06	0.79	0.836	0.550	0.016	0.630	0.665	0.041
	(14 or 15)-methylpalmitate (a17:0 or i17:0)	HMDB0061709	5695	269.249	neg	0.77	0.82	0.57	0.058	0.096	0.001	0.361	0.393	0.012
	(16 or 17)-methylstearate (a19:0 or i19:0)	HMDB37397	5993	297.280	neg	0.76	0.82	0.51	0.059	0.050	0.000	0.361	0.374	0.005
Fatty Acid, Dicarboxylate	pimelate (C7-DC)	HMDB00857	2745	159.066	neg	0.67	0.69	0.48	0.260	0.276	0.035	0.463	0.516	0.063
	suberate (C8-DC)	HMDB00893	804.3	173.082	neg	1.01	0.72	0.65	0.879	0.127	0.045	0.641	0.429	0.072
	sebacate (C10-DC)	HMDB00792	1788	201.113	neg	0.71	0.71	0.59	0.013	0.013	0.002	0.357	0.279	0.013
	dodecadienoate (12:2)*		5146	195.139	neg	0.63	0.63	0.55	0.123	0.113	0.044	0.385	0.410	0.071
	dodecanedioate (C12-DC)	HMDB00623	2990	229.145	neg	0.53	0.77	0.61	0.015	0.228	0.022	0.357	0.499	0.047
	tetradecanedioate (C14-DC)	HMDB00872	3985	257.176	neg	0.39	0.66	0.51	0.050	0.363	0.151	0.361	0.584	0.144
Fatty Acid Metabolism (also BCAA	propionylglycine	HMDB00783	960	130.051	neg	1.32	1.48	2.53	0.236	0.164	0.029	0.460	0.453	0.058
Metabolism)	methylmalonate (MMA)	HMDB00202	3078.4	117.019	neg	1.01	0.93	0.66	0.854	0.498	0.021	0.632	0.647	0.046
Fatty Acid Metabolism (Acyl Glycine)	hexanoylglycine	HMDB00701	2900	172.098	neg	0.56	0.55	0.58	0.028	0.025	0.040	0.357	0.317	0.066
Fatty Acid Metabolism (Acyl Carnitine)	laurylcarnitine (C12)	HMDB02250	1235	344.280	pos	0.84	0.67	0.94	0.349	0.039	0.746	0.515	0.364	0.373
	myristoylcarnitine (C14)	HMDB05066	1350	372.311	pos	0.66	0.58	0.71	0.033	0.003	0.038	0.357	0.230	0.065
	palmitoylcarnitine (C16)	HMDB00222	1425	400.342	pos	0.76	0.68	0.83	0.087	0.013	0.176	0.374	0.279	0.158
	palmitoleoylcarnitine (C16:1)*	HMDB0013207	1357	398.326	pos	0.55	0.54	0.59	0.011	0.005	0.009	0.357	0.230	0.029
	stearoylcarnitine (C18)	HMDB00848	1485	428.373	pos	0.86	0.77	0.95	0.221	0.045	0.630	0.451	0.369	0.340
	linoleoylcarnitine (C18:2)*	HMDB06469	1430	424.342	pos	0.67	0.58	0.79	0.036	0.008	0.172	0.357	0.230	0.156
	linolenoylcarnitine (C18:3)*	HMDB0006469	1310	422.326	pos	0.60	0.53	0.75	0.035	0.007	0.135	0.357	0.230	0.136
	oleoylcarnitine (C18:1)	HMDB05065	1423	426.358	pos	0.65	0.59	0.68	0.036	0.006	0.026	0.357	0.230	0.052
	myristoleoylcarnitine (C14:1)*	HMDB0240588	1316	370.295	pos	0.61	0.52	0.75	0.021	0.001	0.082	0.357	0.230	0.103
	arachidonoylcarnitine (C20:4)	HMDB0006455	1353	448.342	pos	0.68	0.62	0.94	0.067	0.012	0.642	0.369	0.279	0.345
	dihomo-linoleoylcarnitine (C20:2)*		1436	452.373	pos	0.66	0.44	0.57	0.015	0.001	0.014	0.357	0.173	0.037
	pentadecanoylcarnitine (C15)*	HMDB0062517	1362	386.326	pos	0.70	0.56	0.71	0.190	0.042	0.215	0.443	0.369	0.178
Fatty Acid Metabolism (Acyl Choline)	arachidonoylcholine	HMDB0240583	1390	390.337	pos	0.69	0.90	0.46	0.212	0.727	0.031	0.451	0.740	0.059
Fatty Acid, Monohydroxy	2-hydroxyoctanoate	HMDB02264	3736.8	159.103	neg	0.91	0.75	0.82	0.228	0.010	0.089	0.451	0.276	0.110
	2-hydroxydecanoate	HMDB0094656	4840	187.134	neg	0.81	0.82	0.72	0.076	0.189	0.022	0.374	0.478	0.047

	3-hydroxyhexanoate		1725	131.071	neg	0.74	0.73	0.60	0.117	0.095	0.017	0.380	0.391	0.042
	3-hydroxysebacate	HMDB00350	1282	217.108	neg	0.53	0.67	0.59	0.008	0.054	0.018	0.357	0.374	0.043
	5-hydroxyhexanoate	HMDB00525	1267	131.071	neg	0.59	0.61	0.52	0.006	0.017	0.003	0.357	0.279	0.016
	8-hydroxyoctanoate	HMDB61914	2300	159.103	neg	0.80	0.67	0.54	0.366	0.134	0.030	0.521	0.435	0.058
	16-hydroxypalmitate	HMDB06294	5236.2	271.228	neg	0.62	0.70	0.49	0.146	0.276	0.039	0.406	0.516	0.065
	13-HODE + 9-HODE		5275	295.228	neg	0.58	0.60	0.42	0.079	0.095	0.009	0.374	0.391	0.029
	14-HDoHE/17-HDoHE	HMDB0060044	5296	343.228	neg	0.54	0.97	0.96	0.029	0.839	0.738	0.357	0.777	0.373
	3-hydroxystearate		5674	299.259	neg	0.68	0.56	0.29	0.215	0.061	0.002	0.451	0.378	0.014
Fatty Acid, Dihydroxy	9,10-DiHOME	HMDB04704	5180	313.238	neg	0.65	0.66	0.56	0.101	0.103	0.048	0.374	0.403	0.074
Eicosanoid	12-HETE	HMDB06111	5326	319.228	neg	0.61	0.65	0.58	0.054	0.048	0.004	0.361	0.374	0.018
Endocannabinoid	oleoyl ethanolamide	HMDB02088	6450	324.291	neg	1.03	0.91	0.54	0.794	0.561	0.004	0.623	0.667	0.018
	palmitoyl ethanolamide	HMDB02100	6300	298.275	neg	0.93	0.89	0.66	0.344	0.313	0.001	0.515	0.548	0.012
	N-oleoyltaurine		5610	388.253	neg	0.82	0.80	0.62	0.308	0.263	0.027	0.488	0.507	0.055
	linoleoyl ethanolamide	HMDB12252	6150	322.275	neg	0.94	0.89	0.43	0.539	0.404	0.000	0.575	0.590	0.006
Inositol Metabolism	1-stearoyl-2-oleoyl-GPC (18:0/18:1)	HMDB08038	2644	788.616	pos	0.79	0.80	0.76	0.159	0.144	0.024	0.421	0.443	0.050
	1-palmitoyl-2-arachidonoyl-GPE (16:0/20:4)*	HMDB05323	2198	740.522	pos	0.51	0.23	0.22	0.251	0.033	0.032	0.461	0.330	0.059
	1-palmitoyl-GPE (16:0)	HMDB11503	1544	454.293	pos	0.57	0.51	0.36	0.100	0.053	0.010	0.374	0.374	0.030
	1-stearoyl-GPE (18:0)	HMDB11130	1626	482.324	pos	0.55	0.43	0.35	0.060	0.016	0.005	0.361	0.279	0.020
Phosphatidylethanolamine (PE) Lysophospholipid	2-stearoyl-GPE (18:0)*	HMDB11129	6350	480.310	neg	0.53	0.57	0.34	0.058	0.082	0.006	0.361	0.391	0.022
	1-oleoyl-GPE (18:1)	HMDB11506	1554	480.308	pos	0.47	0.36	0.29	0.034	0.008	0.003	0.357	0.230	0.016
	1-linoleoyl-GPE (18:2)*	HMDB11507	1482	478.293	pos	0.46	0.33	0.36	0.021	0.004	0.006	0.357	0.230	0.022
	1-arachidonoyl-GPE (20:4n6)*	HMDB11517	1470	502.293	pos	0.50	0.41	0.33	0.026	0.008	0.004	0.357	0.230	0.018
	1-stearoyl-GPI (18:0)	HMDB61696	5794	599.320	neg	1.01	1.07	0.70	0.738	0.582	0.016	0.614	0.679	0.041
Plasmalogen	1-(1-enyl-palmitoyl)-2-palmitoyl-GPC (P-16:0/16:0)*	HMDB11206	2454	718.575	pos	0.77	0.73	0.40	0.204	0.258	0.001	0.451	0.507	0.008
	1-(1-enyl-palmitoyl)-2-arachidonoyl-GPE (P-16:0/20:4)*	HMDB11352	2270	724.528	pos	0.55	0.38	0.31	0.144	0.035	0.015	0.406	0.345	0.040
	1-(1-enyl-palmitoyl)-2-oleoyl-GPC (P-16:0/18:1)*		2443	744.590	pos	0.79	0.65	0.59	0.158	0.005	0.020	0.421	0.230	0.046

	1-(1-enyl-palmitoyl)-2-arachidonoyl-GPC (P-16:0/20:4)*	HMDB11220	2154	766.575	pos	0.84	0.85	0.72	0.124	0.115	0.001	0.385	0.414	0.011
Lysoplasmalogen	1-(1-enyl-palmitoyl)-GPC (P-16:0)*	HMDB10407	1547	480.345	pos	0.87	0.87	0.78	0.069	0.071	0.011	0.369	0.391	0.031
	1-(1-enyl-palmitoyl)-GPE (P-16:0)*		6285	436.283	neg	0.68	0.47	0.39	0.222	0.025	0.010	0.451	0.317	0.031
	1-(1-enyl-oleoyl)-GPE (P-18:1)*		6250	462.299	neg	0.52	0.31	0.31	0.187	0.030	0.024	0.441	0.323	0.050
	1-(1-enyl-stearoyl)-GPE (P-18:0)*		6500	464.315	neg	0.53	0.43	0.39	0.090	0.031	0.021	0.374	0.323	0.046
Glycerolipid	glycerol	HMDB00131	758	91.040	neg	0.86	0.65	0.53	0.301	0.011	0.009	0.483	0.279	0.029
Monoacylglycerol	1-arachidonylglycerol (20:4)	HMDB11549	6250	303.233	neg	0.70	0.88	0.47	0.295	0.786	0.031	0.482	0.762	0.059
Diacylglycerol	linoleoyl-linoleoyl-glycerol (18:2/18:2) [1]*	HMDB07248	2720	634.541	pos	0.71	0.39	0.54	0.319	0.044	0.120	0.496	0.369	0.127
	oleoyl-arachidonoyl-glycerol (18:1/20:4) [1]*	HMDB07228	2907	660.556	pos	0.67	0.70	0.35	0.366	0.434	0.039	0.521	0.606	0.065
Ceramides (Cer)	N-palmitoyl-sphingosine (d18:1/16:0)	HMDB04949	2893	538.519	pos	0.71	0.74	0.55	0.059	0.112	0.005	0.361	0.408	0.020
	ceramide (d18:2/24:1, d18:1/24:2)*		3858	646.613	pos	0.86	0.82	0.54	0.274	0.241	0.015	0.471	0.502	0.039
Hexosylceramides (HCER)	glycosyl-N-palmitoyl-sphingosine (d18:1/16:0)		2623	700.572	pos	0.70	0.69	0.39	0.413	0.372	0.035	0.539	0.585	0.063
Dihydrosphingomyelins	palmitoyl dihydrosphingomyelin (d18:0/16:0)*		2290	705.591	pos	0.73	0.72	0.65	0.007	0.027	0.001	0.357	0.322	0.011
Sphingomyelins (SM)	palmitoyl sphingomyelin (d18:1/16:0)		2168	703.575	pos	0.77	0.75	0.67	0.023	0.039	0.000	0.357	0.364	0.005
	hydroxypalmitoyl sphingomyelin (d18:1/16:0(OH))**		2056	719.570	pos	0.86	0.75	0.70	0.147	0.062	0.038	0.406	0.381	0.065
	stearoyl sphingomyelin (d18:1/18:0)	HMDB01348	2400	731.606	pos	0.70	0.77	0.66	0.016	0.068	0.004	0.357	0.391	0.019
	behenoyl sphingomyelin (d18:1/22:0)*	HMDB12103	3083	787.669	pos	0.84	0.90	0.75	0.068	0.285	0.000	0.369	0.519	0.005
	tricosanoyl sphingomyelin (d18:1/23:0)*	HMDB12105	3200	801.684	pos	0.85	0.88	0.78	0.035	0.209	0.001	0.357	0.495	0.011
	lignoceroyl sphingomyelin (d18:1/24:0)		3437	815.700	pos	0.85	0.88	0.76	0.044	0.104	0.000	0.361	0.403	0.005
	sphingomyelin (d18:2/23:1)*		2315	797.653	pos	0.95	0.83	0.69	0.547	0.311	0.007	0.575	0.547	0.022
	sphingomyelin (d18:2/24:2)*		2215	809.653	pos	0.86	0.82	0.65	0.095	0.093	0.001	0.374	0.391	0.008
	sphingomyelin (d18:1/14:0, d16:1/16:0)*	HMDB12097	1998	675.544	pos	0.69	0.73	0.60	0.030	0.070	0.002	0.357	0.391	0.014
	sphingomyelin (d17:1/16:0, d18:1/15:0, d16:1/17:0)*		2082	689.559	pos	0.84	0.76	0.67	0.109	0.044	0.002	0.380	0.369	0.013

		sphingomyelin (d18:2/16:0, d18:1/16:1)*		2002	701.559	pos	0.81	0.71	0.61	0.043	0.007	0.000	0.361	0.230	0.005
		sphingomyelin (d18:1/17:0, d17:1/18:0, d19:1/16:0)		2312	717.591	pos	0.93	0.85	0.74	0.382	0.108	0.005	0.526	0.407	0.020
		sphingomyelin (d18:1/18:1, d18:2/18:0)	HMDB12101	2167	729.591	pos	0.72	0.71	0.63	0.017	0.031	0.000	0.357	0.323	0.005
		sphingomyelin (d18:1/19:0, d19:1/18:0)*		2330	745.622	pos	0.73	0.58	0.31	0.088	0.046	0.000	0.374	0.369	0.005
		sphingomyelin (d18:1/20:0, d16:1/22:0)*	HMDB12102	2685	759.638	pos	0.79	0.88	0.73	0.062	0.309	0.002	0.361	0.546	0.014
		sphingomyelin (d18:1/20:1, d18:2/20:0)*		2383	757.622	pos	0.74	0.73	0.57	0.039	0.066	0.001	0.361	0.391	0.012
		sphingomyelin (d18:1/20:2, d18:2/20:1, d16:1/22:2)*		2039	755.606	pos	0.58	0.76	0.46	0.069	0.261	0.017	0.369	0.507	0.041
		sphingomyelin (d18:1/21:0, d17:1/22:0, d16:1/23:0)*		2793	773.653	pos	0.90	0.89	0.78	0.383	0.396	0.036	0.526	0.590	0.063
		sphingomyelin (d18:1/22:1, d18:2/22:0, d16:1/24:1)*	HMDB12104	2666	785.653	pos	0.79	0.79	0.67	0.026	0.042	0.001	0.357	0.369	0.011
		sphingomyelin (d18:1/22:2, d18:2/22:1, d16:1/24:2)*		2209	783.637	pos	0.80	0.78	0.68	0.062	0.109	0.003	0.361	0.407	0.016
		sphingomyelin (d18:2/23:0, d18:1/23:1, d17:1/24:1)*		2845	799.669	pos	0.92	0.85	0.76	0.213	0.135	0.000	0.451	0.435	0.006
		sphingomyelin (d18:1/24:1, d18:2/24:0)*	HMDB12107	3033	813.684	pos	0.80	0.82	0.69	0.032	0.061	0.001	0.357	0.378	0.011
		sphingomyelin (d18:2/24:1, d18:1/24:2)*	HMDB0240615	2635	811.669	pos	0.86	0.81	0.76	0.083	0.058	0.003	0.374	0.378	0.017
	Mevalonate Metabolism	3-hydroxy-3-methylglutarate	HMDB00355	2850	161.046	neg	0.82	0.70	0.57	0.452	0.142	0.036	0.555	0.440	0.063
		mevalonolactone	HMDB06024	1375	131.070	pos	0.65	0.73	0.77	0.039	0.008	0.069	0.361	0.230	0.091
	Sterol	cholesterol	HMDB00067	2707	369.352	pos	0.86	0.93	0.66	0.267	0.521	0.001	0.467	0.647	0.012
		beta-sitosterol	HMDB00852	3054	397.383	pos	0.59	0.79	0.42	0.068	0.266	0.000	0.369	0.507	0.005
		campesterol	HMDB02869	2873	383.367	pos	0.56	0.79	0.43	0.083	0.282	0.006	0.374	0.516	0.022
	Corticosteroids	corticosterone	HMDB01547	981	347.222	pos	0.71	0.67	0.55	0.015	0.006	0.003	0.357	0.230	0.018
	Primary Bile Acid Metabolism	tauro-alpha-muricholate		4745	514.284	neg	0.94	1.05	1.61	0.951	0.922	0.036	0.663	0.797	0.063
		deoxycholate	HMDB00626	5294	391.285	neg	0.55	0.67	0.58	0.045	0.189	0.099	0.361	0.478	0.117
	Secondary Bile Acid Metabolism	ursodeoxycholate	HMDB00946	5055	391.285	neg	0.62	0.79	1.06	0.034	0.152	0.954	0.357	0.448	0.423
		hyocholate	HMDB00760	5046	407.280	neg	0.29	0.53	0.47	0.018	0.212	0.124	0.357	0.496	0.129
Nucleotide	Purine Metabolism,	xanthosine	HMDB00299	1075	283.068	neg	0.97	0.68	0.60	0.803	0.081	0.030	0.624	0.391	0.058

	(Hypo)Xanthine/Inosine containing														
	Purine Metabolism, Adenine containing	adenosine 3',5'-cyclic monophosphate (cAMP)	HMDB00058	1952.2	328.045	neg	1.28	0.75	2.87	0.586	0.626	0.021	0.589	0.710	0.046
		1-methyladenine	HMDB11599	2133	150.077	pos	0.58	0.45	0.37	0.027	0.003	0.002	0.357	0.230	0.014
		N1-methyladenosine	HMDB03331	2120	282.120	pos	1.03	0.90	0.87	0.502	0.016	0.003	0.562	0.279	0.017
		N6-succinyladenosine	HMDB00912	940	382.100	neg	1.67	1.71	2.36	0.228	0.156	0.004	0.451	0.448	0.018
	Purine Metabolism, Guanine containing	7-methylguanine	HMDB00897	1729.7	164.058	neg	0.95	0.96	0.83	0.468	0.445	0.022	0.555	0.611	0.047
	Pyrimidine Metabolism, Orotate containing	N-carbamoylaspartate	HMDB00828	3800	175.036	neg	0.66	0.56	0.35	0.093	0.030	0.002	0.374	0.323	0.013
		dihydroorotate	HMDB03349	1910	157.025	neg	0.76	0.62	0.41	0.426	0.146	0.017	0.549	0.443	0.041
		orotate	HMDB00226	1638.1	155.010	neg	0.75	0.65	0.46	0.231	0.064	0.005	0.455	0.387	0.020
	Pyrimidine Metabolism, Uracil containing	5,6-dihydrouridine	HMDB0000497	1119	245.078	neg	0.92	0.95	0.82	0.020	0.095	0.002	0.357	0.391	0.013
		5-methyluridine (ribothymidine)	HMDB00884	1778.1	257.078	neg	0.77	0.73	0.71	0.020	0.018	0.013	0.357	0.279	0.035
		N-acetyl-beta-alanine	HMDB0061880	773	130.051	neg	0.58	1.04	0.75	0.025	0.831	0.178	0.357	0.777	0.159
		3-(3-amino-3-carboxypropyl)uridine*		1369	344.110	neg	0.90	0.92	0.74	0.318	0.432	0.004	0.496	0.606	0.018
	Pyrimidine Metabolism, Cytidine containing	cytidine	HMDB00089	2124	244.093	pos	1.25	1.17	1.26	0.022	0.059	0.016	0.357	0.378	0.041
Cofactors and		quinolinate	HMDB00232	845	168.029	pos	1.52	1.80	1.62	0.041	0.012	0.013	0.361	0.279	0.035
Vitamins		nicotinamide	HMDB01406	1942	123.055	pos	1.14	1.23	1.60	0.196	0.061	0.002	0.451	0.378	0.013
	Nicotinate and Nicotinamide Metabolism	nicotinamide N-oxide	HMDB02730	877	139.050	pos	1.76	1.27	1.89	0.020	0.120	0.006	0.357	0.419	0.022
		1-methylnicotinamide	HMDB00699	1940	137.071	pos	1.18	1.56	2.04	0.380	0.351	0.016	0.526	0.577	0.041
		N1-Methyl-2-pyridone-5-carboxamide	HMDB04193	1668	151.051	neg	1.49	1.33	1.33	0.123	0.151	0.000	0.385	0.448	0.007
		N1-Methyl-4-pyridone-3-carboxamide	HMDB04194	1260	153.066	pos	1.23	1.17	1.18	0.170	0.373	0.022	0.425	0.585	0.047
	Tetrahydrobiopterin Metabolism	biopterin	HMDB00468	1398	236.079	neg	1.05	1.25	1.44	0.634	0.102	0.006	0.606	0.401	0.021
	Hemoglobin and Porphyrin Metabolism	protoporphyrin IX	HMDB00241	1417	563.265	pos	0.36	0.18	0.14	0.049	0.002	0.001	0.361	0.230	0.011
		heme	HMDB03178	1124	616.176	pos	0.56	0.38	0.43	0.059	0.006	0.032	0.361	0.230	0.059
	Vitamin B6 Metabolism	pyridoxal	HMDB01545	2343	168.066	pos	1.04	1.41	1.35	0.752	0.027	0.094	0.615	0.322	0.112
Xenobiotics		hippurate	HMDB00714	2106.9	178.051	neg	0.88	0.68	0.44	0.574	0.077	0.003	0.585	0.391	0.016
	Benzoate Metabolism	3-hydroxyhippurate	HMDB06116	1687	194.046	neg	1.58	1.64	2.15	0.027	0.019	0.009	0.357	0.279	0.029
		catechol sulfate	HMDB59724	1906	188.986	neg	0.45	0.44	0.34	0.101	0.089	0.040	0.374	0.391	0.066
		4-methylcatechol sulfate		2665	203.002	neg	1.20	0.86	0.41	0.316	0.596	0.013	0.496	0.689	0.036

Food Component/Plant	phenylpropionylglycine	HMDB00860	2945	206.082	neg	0.54	0.31	0.32	0.082	0.004	0.009	0.374	0.230	0.029
	3-(3-hydroxyphenyl)propionate sulfate		1294	245.013	neg	3.40	2.61	1.80	0.013	0.027	0.828	0.357	0.322	0.393
	3-(3-hydroxyphenyl)propionate	HMDB00375	1980	165.056	neg	1.93	1.87	1.51	0.007	0.017	0.285	0.357	0.279	0.210
	2-isopropylmalate	HMDB00402	2605	175.061	neg	0.76	0.56	0.51	0.374	0.068	0.045	0.526	0.391	0.072
	equol glucuronide		3215	417.119	neg	0.68	0.91	0.44	0.199	0.632	0.013	0.451	0.716	0.035
	ferulic acid 4-sulfate	HMDB29200	1200	273.007	neg	0.63	0.66	0.25	0.213	0.246	0.004	0.451	0.506	0.018
	histidine betaine (hercynine)*	HMDB0029422	2094	198.124	pos	0.63	0.69	0.56	0.019	0.088	0.020	0.357	0.391	0.046
	homostachydrine*	HMDB33433	1750	158.118	pos	1.13	1.14	1.31	0.215	0.243	0.024	0.451	0.502	0.050
	3-hydroxycinnamate sulfate		1338	242.997	neg	3.10	2.79	1.71	0.012	0.019	0.690	0.357	0.279	0.358
	4-hydroxycinnamate	HMDB02035	1457	163.040	neg	0.47	0.60	0.21	0.059	0.173	0.002	0.361	0.453	0.015
	caffeic acid sulfate	HMDB41708	1307	258.992	neg	0.69	0.99	0.51	0.097	0.789	0.002	0.374	0.762	0.013

Table S7. List of significantly changed plasma lipid metabolites in male rats exposed by gavage to boron at 0, 25, 50 and 100 mg/kg/day for 28 days using untargeted lipidomics.

Sub Pathway	Compound	HMDB	M/Z	RT	Mode	Fold of Change			*P* Value			*FDR*		
						25	50	100	25	50	100	25	50	100
Ceramides (Cer)	Cer(d18:1/23:0)	HMDB0000950	694.64	20.30	neg	0.79	0.85	0.75	0.281	0.168	0.010	0.281	0.168	0.010
	Cer(d18:1/24:0)	HMDB0004956	708.65	21.09	neg	0.66	0.80	0.64	0.050	0.053	0.003	0.050	0.054	0.003
	Cer(d18:1/24:1)	HMDB0004953	706.64	19.31	neg	0.67	0.76	0.57	0.084	0.070	0.002	0.085	0.071	0.002
	Cer(d18:2/24:0)	-	706.64	19.58	neg	0.74	0.74	0.53	0.217	0.096	0.007	0.218	0.097	0.007
	Cer(d18:1/16:0)	HMDB0004949	538.52	14.64	pos	0.84	0.85	0.63	0.309	0.309	0.042	0.309	0.310	0.042
	Cer(d18:1/22:0)	HMDB0004952	622.61	19.47	pos	0.83	0.93	0.74	0.306	0.365	0.007	0.307	0.367	0.007
	Cer(d18:2/22:0)	-	620.60	17.95	pos	0.83	0.91	0.67	0.449	0.363	0.009	0.450	0.364	0.009
	Cer(d18:2/24:1)	-	646.61	17.81	pos	0.79	0.84	0.72	0.194	0.084	0.000	0.195	0.084	0.000
Coenzyme (Co)	Co(Q9)	HMDB0006707	812.66	20.93	pos	0.80	0.86	0.76	0.284	0.011	0.026	0.285	0.011	0.026
Diacylglycerol (DG)	DG(16:0/20:4)	HMDB0007112	634.54	15.50	pos	0.87	0.65	0.53	0.547	0.054	0.043	0.548	0.055	0.043
	DG(18:1/18:3)	HMDB0007191	634.54	15.08	pos	0.73	0.46	0.62	0.429	0.034	0.292	0.430	0.034	0.293
Fatty Acids (FA)	FA(16:2)	-	251.20	2.04	neg	0.73	0.66	0.52	0.110	0.070	0.025	0.111	0.070	0.025
	FA(17:1)	HMDB0062437	267.23	8.19	neg	2.84	1.69	2.07	0.050	0.044	0.197	0.050	0.045	0.198
	FA(17:2)	-	265.22	2.45	neg	0.69	0.64	0.47	0.104	0.084	0.027	0.105	0.086	0.028
	FA(18:1)	-	281.25	4.35	neg	0.80	0.69	0.51	0.172	0.074	0.014	0.173	0.074	0.014
	FA(18:2)	-	279.23	3.01	neg	0.87	0.74	0.59	0.241	0.052	0.006	0.241	0.053	0.006
	FA(18:3)	-	277.22	2.26	neg	0.74	0.64	0.46	0.100	0.059	0.012	0.100	0.059	0.012
	FA(18:4)	-	275.20	1.84	neg	0.68	0.67	0.38	0.077	0.130	0.010	0.079	0.130	0.010
	FA(19:0)	-	297.28	7.65	neg	1.12	0.95	0.82	0.318	0.316	0.002	0.319	0.317	0.002
	FA(19:1)	-	295.26	9.91	neg	3.08	1.83	2.21	0.045	0.051	0.177	0.047	0.052	0.178
	FA(20:1)	-	309.28	6.67	neg	0.85	0.76	0.46	0.184	0.054	0.001	0.185	0.054	0.001
	FA(20:2)	HMDB0061864	307.26	4.81	neg	0.86	0.70	0.54	0.222	0.066	0.001	0.223	0.066	0.001
	FA(20:3)	HMDB0002925	305.25	3.48	neg	0.95	0.85	0.60	0.741	0.381	0.007	0.743	0.382	0.008
	FA(20:5)	-	301.22	2.11	neg	1.03	1.00	0.64	0.840	0.999	0.031	0.842	0.999	0.031
	FA(22:0)	-	339.33	10.59	neg	0.99	0.96	0.72	0.918	0.829	0.025	0.920	0.831	0.026

	FA(22:4)	-	331.26	4.06	neg	1.19	1.04	0.73	0.314	0.789	0.028	0.315	0.790	0.028
	FA(22:5)	-	329.25	2.99	neg	1.21	1.06	0.69	0.171	0.757	0.026	0.171	0.758	0.026
	FA(22:6)	-	327.23	2.35	neg	1.10	1.06	0.76	0.548	0.695	0.036	0.549	0.695	0.036
	FA(24:0)	-	367.36	12.62	neg	0.95	1.03	0.71	0.719	0.873	0.021	0.721	0.875	0.022
	FA(24:1)	-	365.34	10.53	neg	0.94	0.97	0.64	0.751	0.896	0.036	0.752	0.896	0.037
	FA(26:1)	-	393.37	12.53	neg	0.72	0.97	0.48	0.121	0.927	0.014	0.122	0.929	0.015
	FA(30:1)	-	449.44	16.20	neg	0.58	0.87	0.33	0.015	0.555	0.001	0.016	0.556	0.001
Lysophospholipid	LPC(16:1)	HMDB0010383	494.32	1.95	pos	1.51	1.14	1.34	0.145	0.227	0.027	0.146	0.228	0.027
(LysoPC)	LPC(18:0)	HMDB0010384	524.37	4.42	pos	1.40	1.07	1.24	0.103	0.463	0.049	0.103	0.464	0.049
Phosphatidylcholine (PC)	PC(15:0/18:1)	HMDB0007938	804.58	13.62	neg	1.22	1.16	1.32	0.119	0.207	0.037	0.120	0.207	0.037
	PC(15:0/20:3)	HMDB0007947	828.58	12.73	neg	1.27	1.20	1.24	0.095	0.042	0.006	0.095	0.043	0.006
	PC(16:0/16:0)	HMDB0000564	792.58	14.29	neg	1.29	1.11	1.29	0.193	0.207	0.003	0.194	0.207	0.003
	PC(16:0e/18:2)	HMDB0011151	802.60	14.16	neg	1.06	0.95	1.15	0.686	0.655	0.035	0.688	0.655	0.035
	PC(16:0p/18:1)	HMDB0007997	802.60	15.11	neg	0.75	0.70	0.80	0.034	0.008	0.147	0.036	0.008	0.147
	PC(17:0/20:3)	-	856.61	14.20	neg	1.22	1.15	1.22	0.074	0.086	0.009	0.074	0.088	0.009
	PC(18:0/20:3)	HMDB0008046	870.62	15.52	neg	1.72	1.70	1.74	0.039	0.074	0.056	0.040	0.074	0.056
	PC(18:0/20:4)	HMDB0008048	868.61	14.34	neg	1.12	1.16	1.17	0.063	0.024	0.077	0.064	0.024	0.078
	PC(18:1/18:1)	HMDB0000593	844.61	14.63	neg	0.96	1.03	1.16	0.360	0.774	0.048	0.362	0.776	0.049
	PC(20:1/18:2)	HMDB0008303	870.62	14.57	neg	1.10	1.16	1.15	0.102	0.052	0.009	0.102	0.052	0.009
	PC(15:0/16:0)	HMDB0007935	720.55	13.53	pos	1.39	1.22	1.17	0.067	0.091	0.041	0.069	0.092	0.042
	PC(15:0/20:4)	HMDB0007949	768.55	11.98	pos	1.31	1.27	1.20	0.050	0.008	0.020	0.050	0.009	0.020
	PC(16:0/12:0)	-	678.51	10.96	pos	1.65	1.26	1.38	0.111	0.121	0.009	0.113	0.122	0.009
	PC(16:0/18:1)	HMDB0007971	760.59	14.34	pos	1.20	1.14	1.17	0.096	0.038	0.012	0.098	0.039	0.012
	PC(16:0/18:2)	HMDB0007973	758.57	13.10	pos	1.17	1.11	1.18	0.183	0.188	0.009	0.184	0.189	0.009
	PC(16:0/20:4)	HMDB0007982	782.57	12.80	pos	1.28	1.27	1.18	0.085	0.003	0.001	0.085	0.003	0.001
	PC(16:0/22:6)	HMDB0007991	806.57	12.31	pos	1.13	1.18	1.17	0.246	0.045	0.079	0.247	0.046	0.079
	PC(16:0e/20:4)	HMDB0011221	768.59	14.19	pos	1.64	1.71	1.94	0.026	0.137	0.002	0.027	0.138	0.002
	PC(16:1/20:4)	HMDB0008015	780.55	13.10	pos	1.52	1.39	1.47	0.100	0.110	0.018	0.102	0.111	0.018
	PC(16:1/22:6)	HMDB0008023	804.55	12.80	pos	1.45	1.49	1.48	0.132	0.089	0.026	0.133	0.090	0.027
	PC(17:0/20:4)	-	796.59	13.61	pos	1.25	1.21	1.10	0.011	0.017	0.208	0.013	0.018	0.208

	PC(17:1/22:6)	-	818.57	13.61	pos	1.27	1.24	1.12	0.019	0.024	0.222	0.020	0.024	0.222
	PC(18:0/16:0)	HMDB0008034	762.60	15.86	pos	1.08	1.06	1.13	0.119	0.220	0.006	0.119	0.221	0.006
	PC(18:0/18:2)	HMDB0008039	786.60	14.64	pos	1.05	1.08	1.13	0.260	0.190	0.035	0.260	0.190	0.036
	PC(18:0/20:4)	HMDB0008048	810.60	14.33	pos	1.18	1.28	1.14	0.039	0.030	0.184	0.039	0.030	0.185
	PC(18:0/20:5)	HMDB0008050	808.59	14.68	pos	1.25	1.33	1.33	0.077	0.057	0.002	0.077	0.058	0.002
	PC(18:0/22:6)	HMDB0008057	834.60	15.02	pos	0.85	0.90	0.69	0.164	0.190	0.023	0.165	0.192	0.023
	PC(18:0e/20:4)	HMDB0013420	796.62	15.73	pos	1.25	1.29	1.47	0.136	0.058	0.028	0.137	0.059	0.028
	PC(18:0e/22:6)	HMDB0013422	820.62	14.84	pos	1.22	1.28	1.48	0.225	0.109	0.009	0.226	0.110	0.009
	PC(18:0p/20:4)	HMDB0008048	794.61	14.57	pos	1.35	1.30	1.35	0.163	0.077	0.011	0.164	0.079	0.011
	PC(18:1/18:2)	HMDB0008072	784.59	15.85	pos	1.26	1.20	1.31	0.022	0.052	0.005	0.022	0.052	0.005
	PC(18:1/20:4)	HMDB0008081	808.59	15.09	pos	1.33	1.36	1.80	0.054	0.030	0.000	0.055	0.031	0.001
	PC(19:0/20:4)	-	824.62	15.10	pos	1.16	1.24	1.09	0.093	0.027	0.380	0.094	0.028	0.381
	PC(19:1/20:4)	-	822.60	14.17	pos	1.36	1.37	1.37	0.074	0.041	0.047	0.074	0.042	0.048
	PC(20:0/14:4)	-	754.54	11.13	pos	1.44	1.38	1.15	0.169	0.021	0.084	0.170	0.022	0.085
	PC(20:0/20:4)	HMDB0008279	838.63	15.84	pos	1.16	1.34	1.19	0.146	0.034	0.093	0.147	0.035	0.094
	PC(20:0e/22:6)	HMDB0008288	848.65	15.40	pos	1.17	1.18	1.26	0.049	0.139	0.060	0.049	0.140	0.060
Phosphatidylethanolamine	PE(18:1p/22:6)	HMDB0011460	772.53	13.49	neg	0.65	1.04	1.13	0.027	0.730	0.356	0.029	0.732	0.358
(PE)	PE(14:0/14:0)	HMDB0008821	636.46	11.32	pos	1.69	1.22	1.36	0.128	0.130	0.011	0.129	0.131	0.011
	PE(16:0p/20:4)	HMDB0008937	724.53	13.89	pos	1.04	1.16	1.29	0.892	0.440	0.042	0.894	0.441	0.043
	PE(16:0p/22:4)	HMDB0011358	752.56	14.93	pos	0.95	1.17	1.37	0.778	0.401	0.034	0.780	0.403	0.035
	PE(18:0/18:1)	HMDB0008992	746.57	16.15	pos	1.19	1.05	1.40	0.131	0.745	0.001	0.131	0.747	0.001
	PE(18:0p/20:4)	HMDB0009003	752.56	15.37	pos	0.99	1.19	1.35	0.912	0.313	0.016	0.914	0.315	0.016
	PE(18:0p/22:4)	HMDB0011391	780.59	16.42	pos	0.96	1.15	1.34	0.745	0.462	0.038	0.747	0.463	0.038
	PE(18:1/18:2)	HMDB0009027	742.54	13.54	pos	1.20	1.05	1.20	0.164	0.577	0.031	0.164	0.579	0.031
	PE(18:1p/18:2)	HMDB0011442	726.54	14.19	pos	1.15	1.17	1.38	0.291	0.317	0.002	0.293	0.318	0.002
Phosphatidylinositol (PI)	PI(16:0/22:4)	HMDB0009793	885.55	11.29	neg	1.71	0.42	4.62	0.176	0.148	0.000	0.176	0.149	0.000
	PI(16:0/22:6)	-	881.52	9.89	neg	1.34	1.52	1.54	0.432	0.015	0.081	0.433	0.015	0.081
	PI(18:0/20:4)	HMDB0009815	885.55	11.66	neg	0.92	1.10	1.10	0.729	0.099	0.030	0.729	0.100	0.030
	PI(16:0/18:2)	HMDB0009784	852.56	10.47	pos	1.00	1.16	1.25	1.000	0.143	0.016	1.000	0.145	0.016
	PI(16:0/20:4)	HMDB0009789	876.56	10.25	pos	1.02	1.22	1.18	0.946	0.034	0.022	0.948	0.034	0.022

Sphingomyelins (SM)	SM(d16:0/26:1)	-	873.71	20.57	neg	1.24	1.10	1.25	0.103	0.121	0.001	0.104	0.121	0.001
	SM(d18:1/14:0)	HMDB0012097	733.55	10.98	neg	1.02	0.93	0.77	0.920	0.406	0.005	0.922	0.407	0.005
	SM(d20:0/18:2)	-	815.63	14.58	neg	1.59	1.11	1.14	0.022	0.310	0.094	0.024	0.311	0.094
	SM(d16:0/27:4)	-	823.67	18.57	pos	1.19	1.26	1.28	0.102	0.006	0.038	0.103	0.006	0.038
	SM(d16:1/16:0)	HMDB0240616	675.54	10.96	pos	1.06	0.87	0.76	0.851	0.240	0.008	0.853	0.241	0.008
	SM(d16:1/18:1)		701.56	11.16	pos	1.02	0.90	0.81	0.931	0.223	0.044	0.932	0.224	0.044
	SM(d18:1/18:1)	HMDB0012101	729.59	13.22	pos	0.75	0.91	0.85	0.461	0.287	0.045	0.462	0.288	0.046
	SM(d18:1/22:1)	HMDB0012104	785.65	15.94	pos	0.95	0.99	0.89	0.621	0.935	0.027	0.623	0.936	0.027
	SM(d18:1/25:6)	-	817.62	13.06	pos	1.05	1.03	1.14	0.513	0.614	0.005	0.515	0.616	0.005
Sphingoid base (So)	So(d16:0)	-	274.27	1.92	pos	1.01	0.67	1.04	0.973	0.015	0.918	0.975	0.015	0.919
Steroid (StE)	StE(20:4)	HMDB0000827	716.63	22.85	pos	2.17	2.14	2.02	0.003	0.002	0.009	0.004	0.002	0.009
Triacylglycerol (TG)	TG(12:0/18:2/18:2)	-	816.71	22.04	pos	0.69	0.55	0.49	0.149	0.066	0.047	0.149	0.066	0.047
	TG(14:0/18:2/18:3)	HMDB0042527	842.72	22.15	pos	0.47	0.33	0.28	0.081	0.033	0.019	0.083	0.034	0.020
	TG(15:0/18:1/18:2)	HMDB0011708	860.77	22.87	pos	0.79	0.63	0.43	0.412	0.164	0.024	0.413	0.165	0.025
	TG(16:0/14:0/18:1)	HMDB0010414	822.75	22.96	pos	0.75	0.87	0.44	0.223	0.689	0.015	0.224	0.689	0.015
	TG(16:0/14:0/22:6)	HMDB0043855	868.74	22.52	pos	0.58	0.59	0.44	0.050	0.152	0.017	0.052	0.153	0.018
	TG(16:0/16:0/18:1)	HMDB0005360	850.79	23.22	pos	0.75	0.74	0.36	0.209	0.390	0.003	0.210	0.391	0.003
	TG(16:0/16:0/18:2)	HMDB0005362	848.77	22.96	pos	0.73	0.67	0.53	0.150	0.259	0.049	0.152	0.259	0.049
	TG(16:0/16:0/18:3)	HMDB0010417	846.75	22.73	pos	0.70	0.58	0.44	0.300	0.172	0.049	0.300	0.173	0.049
	TG(16:0/18:1/18:1)	HMDB0005382	876.80	23.18	pos	0.76	0.78	0.39	0.349	0.553	0.026	0.349	0.554	0.026
	TG(16:0/18:1/18:2)	HMDB0005384	874.79	23.30	pos	1.22	2.43	4.15	0.409	0.160	0.037	0.410	0.161	0.037
	TG(16:0/18:1/22:6)	HMDB0044135	922.79	22.66	pos	0.75	0.63	0.59	0.171	0.052	0.010	0.172	0.052	0.011
	TG(16:1/14:0/18:1)	HMDB0010420	820.74	22.73	pos	0.70	0.70	0.44	0.230	0.300	0.034	0.231	0.301	0.034
	TG(16:1/16:1/16:1)	HMDB0005432	818.72	22.43	pos	0.49	0.52	0.44	0.040	0.074	0.041	0.042	0.075	0.041
	TG(18:0/16:0/18:1)	HMDB0010431	878.82	23.38	pos	0.61	0.56	0.33	0.100	0.075	0.006	0.100	0.076	0.006
	TG(18:0/18:1/18:1)	HMDB0005403	904.83	23.35	pos	0.71	0.52	0.38	0.173	0.047	0.006	0.174	0.048	0.006
	TG(18:1/18:1/18:1)	HMDB0005453	902.82	23.15	pos	0.74	0.64	0.35	0.139	0.221	0.007	0.139	0.222	0.007
	TG(18:1/18:1/18:2)	HMDB0005455	900.80	22.95	pos	0.60	0.87	0.80	0.017	0.749	0.137	0.019	0.749	0.137
	TG(18:3/18:2/18:2)	-	894.75	22.21	pos	0.49	0.35	0.35	0.040	0.015	0.023	0.040	0.016	0.024
	TG(18:3/18:2/20:4)	HMDB0053058	918.75	22.07	pos	0.76	0.61	0.63	0.241	0.028	0.079	0.242	0.029	0.080

REFERENCES

1. Wilmanski, T.; Rappaport, N.; Earls, J. C.; Magis, A. T.; Manor, O.; Lovejoy, J.; Omenn, G. S.; Hood, L.; Gibbons, S. M.; Price, N. D., Blood metabolome predicts gut microbiome alpha-diversity in humans. *Nature biotechnology* **2019,** *37*, (10), 1217-1228.
2. Tian, Y.; Wang, Z.; Liu, X.; Duan, J.; Feng, G.; Yin, Y.; Gu, J.; Chen, Z.; Gao, S.; Bai, H.; Wan, R.; Jiang, J.; Liu, J.; Zhang, C.; Wang, D.; Han, J.; Zhang, X.; Cai, L.; He, J.; Wang, J., Prediction of Chemotherapeutic Efficacy in Non-Small Cell Lung Cancer by Serum Metabolomic Profiling. *Clinical cancer research : an official journal of the American Association for Cancer Research* **2018,** *24*, (9), 2100-2109.
3. Xu, L.; Wang, X.; Jiao, Y.; Liu, X., Assessment of potential false positives via orbitrap-based untargeted lipidomics from rat tissues. *Talanta* **2018,** *178*, 287-293.